Chemically resistant polymeric jointing grout with environmental impact

DROCHYTKA, R.; HODUL, J.; MÉSZÁROSOVÁ, L.; JAKUBÍK, A.

Construction and building materials
Volume 292, 19 July 2021, 123454, Pages 1-20

ISSN: 0950-0618

DOI: https://doi.org/10.1016/j.conbuildmat.2021.123454

Accepted manuscript

Chemically resistant polymeric jointing grout with environmental impact

Rostislav Drochytka, Jakub Hodul, Lenka Mészárosová, Aleš Jakubík

Abstract. This paper deals with the study of the chemical resistance of polymeric jointing grouts intended for the jointing of elements that are permanently stressed by an aggressive chemical environment, such as elements made of cast basalt, placed in the concrete structures of sewerages. The paper researches three types of epoxy jointing grouts designed for conditions where there is a chemically aggressive environment. The optimal amount of hazardous waste (end product and cement bypass dusts) was incorporated in the developed jointing grouts. As part of chemical resistance monitoring, changes in selected physical and mechanical properties of jointing grouts were monitored and evaluated, including microstructure monitoring after chemical stress. The scanning electron microscopy (SEM) was used for the explanation of bonding effects of the polymer matrix with the filler It was found that the use of hazardous waste is highly effective in polymeric grouts with high chemical resistance; there was no noticeable reduction in the chemical resistance of these jointing grouts compared to the reference grouts.

1. Introduction

At present, there is a large demand for highly chemically resistant jointing grouts, intended primarily for the reconstruction of sewerage networks. A large part of sewerage networks originated not only in Europe, but also in the United States and Canada in the 1950s and 1960s. These sewerages, as well as those that are only 30 years old and with a highly aggressive environment, are currently undergoing extensive reconstruction [1],[2]. The environment in sewerage networks is very specific, and a number of degradation processes take place in it. Biodegradation is one of various polymer degradation routes. It is the process by which organic substances are broken down by microorganisms, such as bacteria, fungi and algae. These microorganisms can degrade the polymers aerobically (producing carbon dioxide and water) or anaerobically (producing carbon dioxide, water and methane) [3].

The newly developed material based on epoxy resin is primarily designed for jointing sewerage pipes. Corrosion of concrete pipes in sewerage networks is caused mainly by the action of hydrogen sulphide (H_2S). Hydrogen sulphide is formed by sulphate-reducing bacteria (SRB) in anaerobic sewer biofilms, i.e. sewerage sediments. From the wastewater (WW), H_2S is emitted into the free space and the level of the WW in the sewerage pipe, where it is oxidised to sulphuric acid (H_2SO_4). This chemical reaction can be described by the following equations [4]:

$$H_2S + 2O_2 \rightarrow SO_4^{2-} + 2H^+ \quad (1)$$

$$2S + 3O_2 + 2H_2O \rightarrow 2SO_4^{2-} + 4H^+ \quad (2)$$

H_2SO_4 causes biogenic sulphate corrosion of concrete remediation pipes (Fig. 1), which leads to expansion, cracking and eventually the total disintegration of concrete sewerage pipes. This is because the primary reaction of sulphate anions with calcium hydroxide present in the cementitious sealant produces gypsum and ettringite at a substantially larger volume, which is the main cause of the cracking and degradation of concrete [5]. Aggressive factors that cause unstable sulphur (sulphide) compounds in sewerage systems are the composition of the WW (biochemical oxygen demand), temperature, pH value, residence time of the water in the sewer network, car cleaners and detergents;

improper storage or disposal of substances, e.g. from industry, preparations for destroying weeds and vermin (pesticides, herbicides and insecticides); fertilisers (nitrogen and sulphur) and de-icing salts. Although the concentration of hydrogen sulphide in sewers varies across time and space (from units to several hundred ppm), H_2S is present everywhere in sewerage networks [6].

The following types of WW located in sewers have been identified: sewage (from households, social facilities, hostels, etc.), industrial (from production processes), urban (municipal; a mixture of sewage and others, typically industrial water, which flows through public sewerage), agricultural (plant and animal production, drainage waters from land improvement), rainwater (rainwater drained by the sewer network) and others (e.g. hospital, cooling, mining). As raw WW is also a potential carrier of pathogenic microorganisms, inhalation, contact and ingestion can endanger human health through water or air pathways [7]. The pH values of municipal WW range between of 6.8–8.0 and contains a wide variety of aggressive substances, such as dissolved inorganic salts, hydrocarbons, phenols, polyphenols, ammoniacal nitrogen, mercury, lead, cyanides, surfactants, detergents and phthalates. The sum of volatile fatty acids, soluble proteins and soluble sugars forms about 30% of the total chemical oxygen demand (COD) of the WW [8].

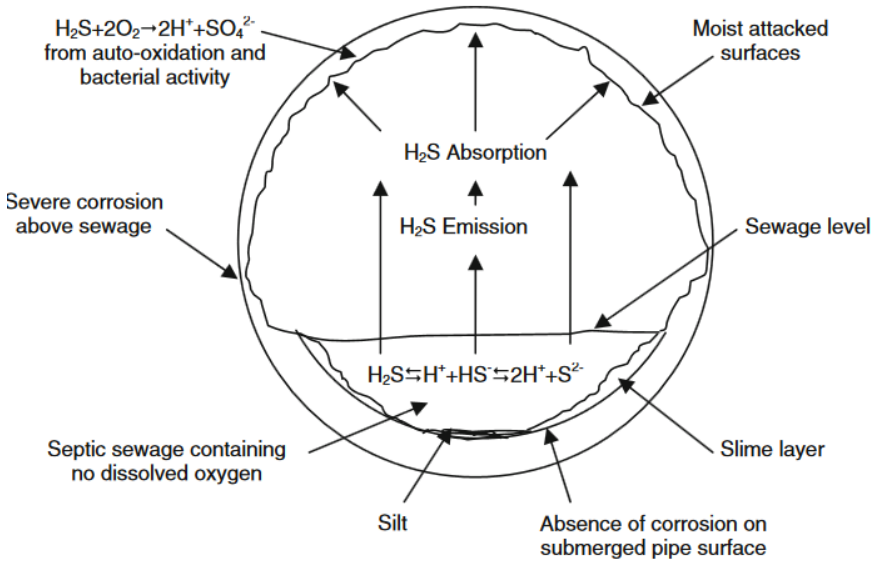

Fig. 1. Scheme of action of aggressive factors on the inner surfaces of sewers [9].

Epoxy resin grouting material has been widely used in foundation treatment and concrete crack treatment because of its good grouting ability and high mechanical strength. It penetrates effectively into porous substrates in a way that provides an embedded network in the material. The main factors that influence grouting quality include durability, permeability and physical and mechanical compatibility. Excellent epoxy grouting materials must have high permeability, good durability and good physical and mechanical compatibility with porous media [10]. The type of curing agent has a significant effect on compressive and flexural strength [11]. The effect of fillers on the ageing of epoxy adhesives has been studied by some authors [12],[13]. The environmental impact of polymer grouts may be assessed by analysis of the life cycle. The environmental impact of polymer composites breaks down to about 70–75% because of extraction, 10–15% because of processing, and 12–18% because of the material itself [14]. However, the environmental impact of using epoxy resins, which exhibit

excellent properties and durability, is much reduced by using hazardous wastes as fillers that are firmly incorporated in the polymer matrix.

In addition to conventional quartz sand or quartz flour, many authors have dealt with alternative preparations of epoxy composite with used filler, e.g. based on kaolinite [15], bentonite [16] and nanosilica [17].

One way to use hazardous waste materials is through their solidification. The principle is to mix the hazardous waste materials with an agent that will guarantee stabilisation. Of course, it is most appropriate to use the maximum possible share of hazardous waste [18],[19]. For the perfect incorporation of hazardous waste in the structure, it is possible to perform two-stage stabilisation. The first step is to mix the waste with a solidifying agent. For the second step, the raw material thus prepared is incorporated in a structure in which it is firmly enclosed. A very suitable material for this purpose is epoxy resin [20]. The key technologies for harmlessly co-disposing and recycling municipal solid waste incinerated fly ash, pickling sludge and waste glass were researched by Zhao et al. [21], and eco-friendly materials using solid wastes as raw materials were formed. It was claimed by Erdoğan et al. [22] that using slag reinforcement in the composite based on epoxy matrix is advantageous both in terms of eliminating wastes that are harmful to the environment and in terms of preserving natural reinforcement sources used in the production of the composite materials.

Stabilisation/solidification (S/S) is an efficient and reliable treatment technology for hazardous materials [23]. The S/S processes can be driven by physical and chemical means, encapsulation, fixation or adsorption with waste components [24]. S/S causes chemical changes in the hazardous components in the waste; these changes reduce solubility, mobility and toxicity [25]. It was proven by Massardier et al. [26] and Vipulanandan [27] that the S/S of hazardous waste by the use of polymeric thermosetting materials is very effective, with the solidified waste having the potential to be used in construction applications.

2. Materials

Three types of two-component epoxy resins (HRG-D, ERG-D, MRG-W) were selected as a binder, quartz flour was used as the reference filler, and further solidified hazardous waste consisting of end product (EP), cement dusts, fly ash and quartz flour.

2.1. Polymer binder

Three types of two-component epoxy resins were used: chemically resistant (HRG-D), highly chemically resistant (ERG-D) and water-compatible resin with average chemical resistance (MRG-W). IN-CHEMIE Technology, Ltd. supplied the HRG-D and ERG-D epoxy resins. The epoxy resin MRG-W was from Redrock Construction, Ltd. The last type of resin (MRG-W) was examined due to the permanently humid environment in the sewers due to the condensation of vapours on the inner walls (drying is technologically and time-consuming). The composition of the resins used is given in Tables 1–3. Densities of the polymer (epoxy) resins and the curing agents, including additives used for the specimen's preparation, are stated in Table 4. The ambient and substrate temperature in the range of 10 ° - 25 ° C must be guaranteed to ensure the required curing of used polymer binders. When applying the materials HRG-D and ERG-D, the maximum moisture content of the substrate must not exceed 5% wt., and relative humidity (R.H.) must be ≤ 80%. For MRG-W resin, the substrate's maximum moisture content must be ≤ 10% wt., and R.H. ≤ 95%. A curing time for the ERG-D and HRG-D binders is 20 hours

at temperature +20 °C, and for MRG-W, the time for complete curing is 24 hours. After mixing the two components (A + B) of polymer binder, the temperature rises during the polymerisation due to the exothermic reaction was: +2.5 ° C after 60 minutes (MRG-W), +10.1 °C (HRG-D), +13.2 °C (ERG-D) after 90 minutes. The filler did not significantly affect the temperature rise during polymerisation (heat mechanism). Dynamic viscosities of used unfilled polymer resins at 23 °C (mixture of A+B components) were 11,100 mPa·s (ERG-D), 5,900 mPa·s (HRG-D) and 1,900 mPa·s with MRG-W binder. The hardener and the thermal curing procedure's type and concentration affect the curing process of epoxy resins. The degree of cure has a high impact on epoxy systems' physical and mechanical properties [28]. Benzyl alcohol (dynamic viscosity 5.84 mPa·s at 20 °C) and a petroleum solvent were present to adjust the viscosity or catalyse the reaction. Benzyl alcohol was used as the solvent in the ERG-D curing agent since it is soluble in the aromatic-containing epoxy resin and dissolves the hydrogen-bonded amine [29]. Cyclohexylamine (dynamic viscosity 2.1 mPa·s at 20 °C) is an interesting compound that, due to its ability as both proton donor and proton acceptor, is used in epoxy systems [30]. The morphology of the epoxy blend cured by primary aliphatic amines, e.g., cyclohexylamine, is influenced by the curing temperature. A higher temperature can reduce the blend viscosity and facilitate easier diffusion of all components [31].

A more complex empirical model proposed by Kenny et al. [32] represents more comprehensively the effect of the degree of cure on the resin viscosity by accounting for the degree of cure at gelation, determined as:

$$\mu = A_\mu exp\left(\frac{E_\mu}{RT}\right)\left[\frac{\alpha_g}{\alpha_g-\alpha}\right]^{(A+B\alpha)} \quad (3)$$

where A_μ, E_μ, A and B are experimentally determined constants, R is the universal gas constant, and α_g is the degree of cure at gelation. As α approaches α_g, the resin viscosity increases dramatically as the polymer system becomes a three-dimensional network.

Table 1

Chemical composition of the chemically resistant epoxy resin HRG-D.

Component A	**Component B (curing agent)**	**Mixing ratio A:B**
ER (average molar mass ≤ 700) (alkoxymethyl) oxirane (C12-C14 alkyl) formaldehyde; oligomeric reaction products with 1-chloro-2,3-epoxypropane and phenol	4,4-methylenebis (cyclohexylamine) Phenylmethanol, formaldehyde polymer with benzenamine	1.8:1

Table 2

Chemical composition of the chemically resistant epoxy resin ERG-D.

Component A	**Component B (curing agent)**	**Mixing ratio A:B**
Polymer with formaldehyde, phenol glycidyl ether, 1- (2,3-epoxypropoxy) -2,2-bis [(2,3-epoxypropoxy) methyl] butane	Benzyl alcohol, m-phenylenebis (methylamine) Phenol 4,4´ (1-methyletathylidene) bis-oligomeric reaction product with 2-(chloromethyl) oxirane reaction product with	2.1:1

	1,3-benzenedimethanamine 4,4´-methylenebis (cyclohexamine)

Table 3

Chemical composition of the water compatible epoxy resin MRG-W

Component A (curing agent)	Component B	Mixing ratio A:B
Formaldehyde, polymer with N1- (2-aminoethyl) -N2-[2-[(2-aminoethyl) amino]ethyl]-1,2-ethanediamine, 2,2´-[1,4-butanediylbis(oxymethyl), polyoxypropylenediamine, 3,6,9-triazaundecane-1,11-diamine	ER (average molar mass ≤ 700), polymer with formaldehyde, polymer with formaldehyde, (alkoxymethyl) oxirane (alkyl C12-C14)	1.16:1.93

Table 4

Densities of the epoxy resins and the curing agents including additives in kg/m^3

Type of Polymer grout	Epoxy resin	Curing agent
ERG-D	1,300	1,100
HRG-D	1,330	1,100
MRG-W	1,270	1,120

2.2. Filler component

Some hazardous wastes, quartz flour and fly ash were selected as by-products as input materials for solidification. In regard to experimental secondary raw material, a mix was used, which was prepared through the homogenisation of quartz powder, hazardous waste as a by-product of solid municipal waste combustion – end product (EP) and cement bypass dust (CBD). Fly ash from fluidised bed combustion (FBC) contaminated by the denitrification process from a thermal power plant in the Czech Republic was used as a solidifying agent together with quartz flour.

2.2.1. Quartz flour

Silica powder is made by grinding dry quartz sand, followed by subsequent selection so that the highest possible quality and low dust content is ensured. It has high mechanical and chemical resistance. The quartz flour used contained SiO_2 over 98.5% and Fe_2O_3 up to 10%, with grain sizes up to 0.2 mm, no organic contamination, specific gravity of 2,680 kg/m^3 and specific surface area of 4,660 cm^2/g. For water-compatible MRG-W grouts, black coloured quartz flour (specific gravity of 2,690 kg/m^3) treated with the addition of Fe_2O_3 (maximum amount 2.0%) was used, which is commonly utilised in practice in these types of materials.

2.2.2. End product (EP)

The EP is a waste product from the II. stage of flue gas treatment of category HW – hazardous. Its chemical composition depends on the composition of the flue gas, i.e. on the composition of mixed municipal waste (MMW). It is separated on textile filters as the final reaction product of the neutralisation reaction of acid components of flue gases and alkaline sorbent – lime wash. It is a very fine dust of dark grey colour (due to the presence of activated carbon), odourless and strongly

hygroscopic due to unreacted $Ca(OH)_2$. The experimentally determined specific weight of the used material was 2,340 kg/m^3, while the specific surface area was 5,190 cm^2/g. The pH value of the aqueous extract of the EP was 12.2. The X-ray diffraction pattern of the EP, with mineral peaks for defernite ($Ca_6(CO_3)_{2-x}(SiO_4)_x(OH)_7(Cl,OH)_{1-2x}$), cuspidine ($Ca_4(Si_2O_7)(F,OH)_2$), portlandite ($Ca(OH)_2$), hannebachite ($2CaSO_3 \cdot H_2O$), high-temperature polymorph of silica with a crystal structure (β-quartz), anhydrite ($CaSO_4$) and calcite ($CaCO_3$), is stated in Fig. 2. The record of the differential thermal analysis (DTA) and thermogravimetric analysis (TGA), with the indication of hydration products decomposition of the EP, is presented in Fig. 3. The blue curve is the thermogravimetric (TG) curve, the red curve represents the first derivative of the TG curve (DTG), and blue dashed curve represents the DTA curve. Table 5 displays the content of minerals and phases calculated based on the DTA and TG record. Table 6 presents the chemical composition of the hazardous waste and fly ash used, including the content of heavy metals in dry matter.

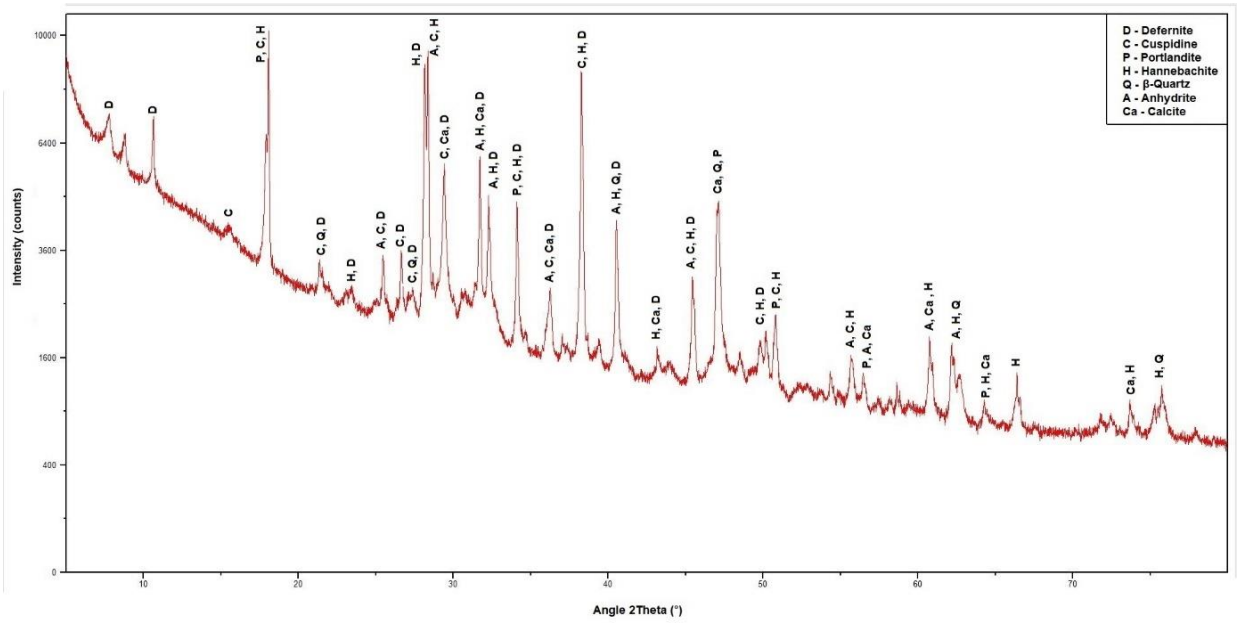

Fig. 2. X-ray diffraction pattern of the end product (EP).

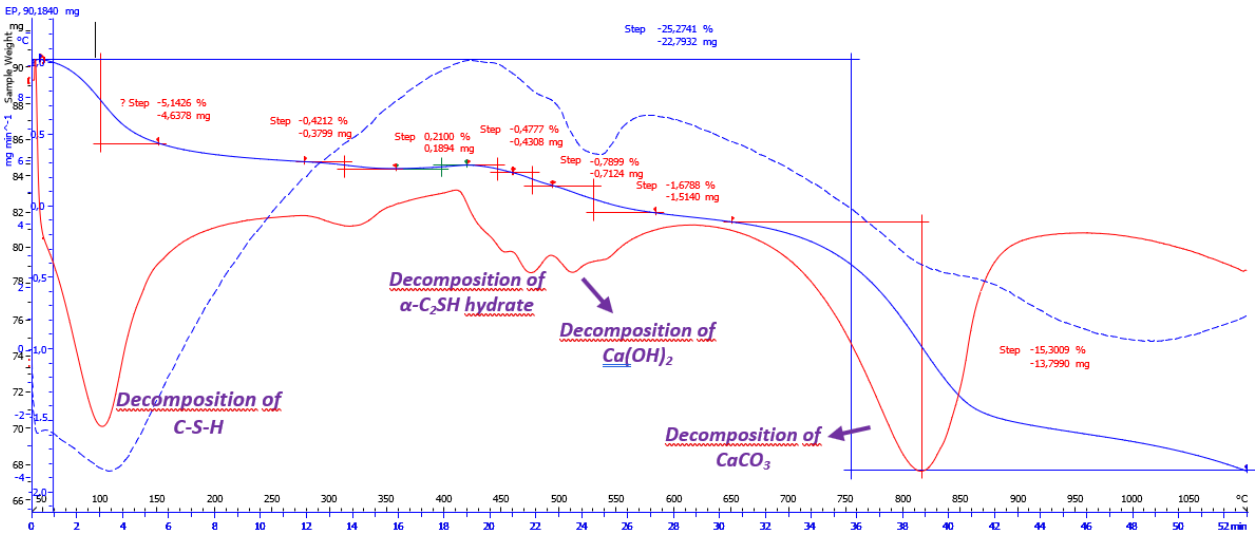

Fig. 3. Thermo-gravimetric and differential thermal analysis curves of the end product (EP) - red curve (DTG), blue dashed curve (DTA) and blue curve (TG).

2.2.3. Cement Bypass Dust (CBD)

CBD is a by-product of the production of cement in cement plants. Due to the high circulation of pollutants (chlorine, alkalis and, to a lesser extent, sulphur), it is important to include a gas bypass at the entrance to the cement kiln. Bypass dusts make up 5–20% of the clinker produced. Typical bypass components are chlorine bypass (up to 15%) and sulphur bypass (up to 70%). The bypass is an exhaust of a part of furnace gases from the transitional part of the rotary cement furnace, rapid cooling of this part of furnace gases and their diverting into an independent filter. These gases are not led to the exchanger before the furnace where partial calcination in the raw material mix takes place. The percentage of coarse fraction is 85–90%, and it can be returned to the cement production process - reduced concentration of chlorides, and fine fraction presents 10–15% of the total amount of dust. The fine fraction used in the research contained a larger amount of chlorides and also contained heavy metals, such as lead, copper and cadmium [33], which is evident from their chemical composition (shown in Table 6). The specific weight was 2,790 kg/m^3, while the specific surface area was 6,440 cm^2/g. The pH value of the aqueous extract of CBD was 12.8. The X-ray diffraction pattern for the CBD, with mineral peaks for syngenite ($K_2Ca(SO_4)_2 \cdot H_2O$), portlandite ($Ca(OH_2)$), belite ($2CaO \cdot SiO_2$), calcite ($CaCO_3$), hydrogrossular ($Ca_3Al_2(SiO_4)_{3-x}(OH)_{4x}$) and sylvine (KCl), can be seen in Fig. 4. The record of the DTA and TGA of CBD is presented in Fig. 5., and the content of minerals and phases calculated based on the DTA and TG record is stated in Table 5.

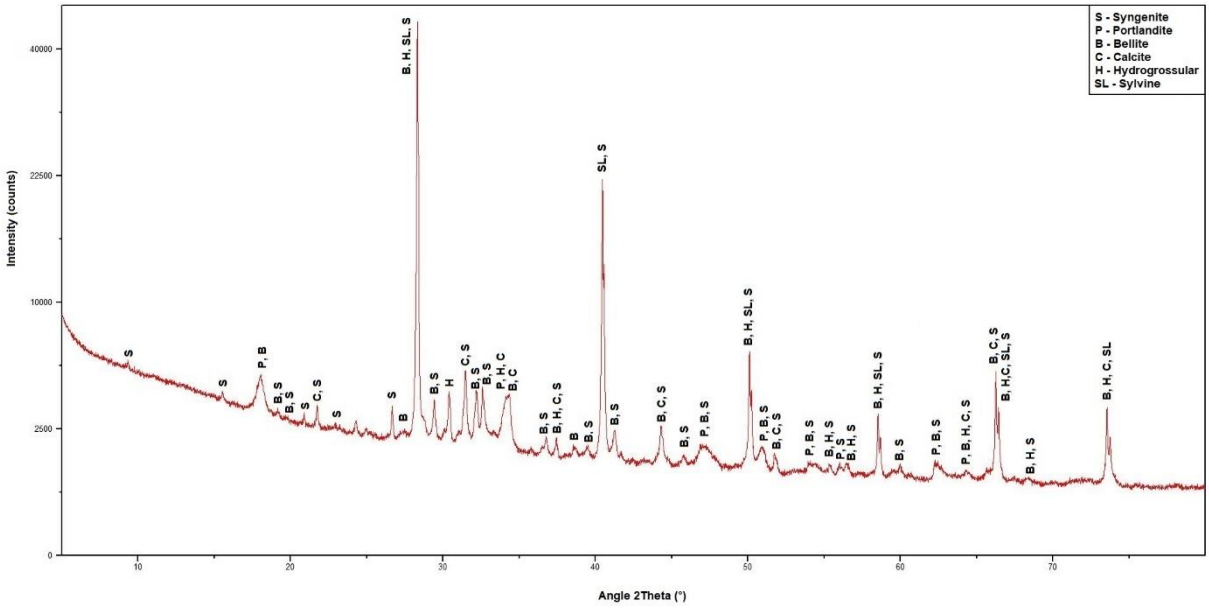

Fig. 4. X-ray diffraction pattern of the cement bypass dust (CBD).

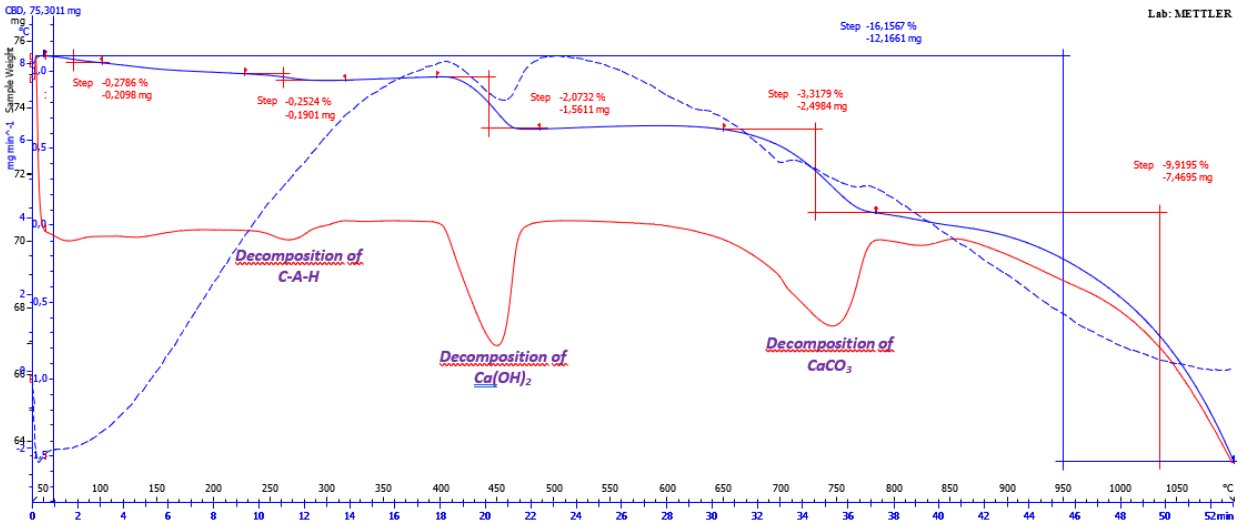

Fig. 5. Thermo-gravimetric and differential thermal analysis curves of the Cement Bypass Dust (CBD).

Table 5

Results of DTA – mass loss and mass content.

Hazardous waste	Mass loss corresponding to decomposition [%]				Mass Content [%]	
	C-S-H	C-A-H	$Ca(OH)_2$	$CaCO_3$	$Ca(OH)_2$	$CaCO_3$
End Product (EP)	5.62	0	2.47	15.3	10.2	34.8
Cement Bypass Dust (CBD)	0	0.25	2.07	3.32	8.5	7.5

2.2.4. Fly Ash from Fluidized Bed Combustion (FBC)

The fly ash from FBC, which was contaminated due to selective non-catalytic reduction (SNCR) technology, is a by-product of a lignite-burning thermal power plant in the west part of the Czech Republic. The specific weight of this material was experimentally determined to be 2,872 kg/m^3, the specific surface area was found to be 627 m^2/kg and the concentration of ammonia ions (NH_3) = 30.11 ppm. As it can be seen from the Table 6, this fly ash contained significant amounts of vanadium (242 mg/kg dry matter) and chromium (91.9 mg/kg dry matter).

Table 6

Chemical composition of hazardous waste and fly ash.

Parameter	Unit	EP	CBD	FBC
Dry matter (105 °C)	%	99.6	99.7	99.8
Chlorides	mg/ kg dry matter	151000	117000	76
Sulphates (SO_4^{2-})	% dry matter	4.20	8.02	5.88
SiO_2	% dry matter	3.81	9.39	35.2
Al_2O_3	% dry matter	1.86	2.13	19.8
CaO	% dry matter	37.8	32.5	18.5
Free CaO	% dry matter	26.9	9.81	8.74
P_2O_5	% dry matter	0.40	0.14	0.18
Fe_2O_3	% dry matter	0.65	1.33	5.80
K_2O	% dry matter	5.52	22.7	0.63
Na_2O	% dry matter	3.29	0.93	0.31
MgO	% dry matter	0.74	0.71	1.05

TiO_2	% dry matter	0.38	0.14	2.27
As	mg/kg dry matter	45.1	16.0	12.4
Cd	mg/kg dry matter	83.7	76.3	<0.40
Cr	mg/kg dry matter	63.1	155.0	91.9
Hg	mg/kg dry matter	12.6	<0.20	<0.20
Ni	mg/kg dry matter	19.3	9.4	87.4
Pb	mg/kg dry matter	1310	3720	17.0
V	mg/kg dry matter	15.2	30.6	242.0
Total Petroleum Hydrocarbons C10–C40	mg/kg dry matter	<20	<20	<20

2.3. Solidification of hazardous waste

In the first stage, the filling component was created as a mix of individual secondary raw materials. The filler in the form solidification product based on hazardous waste (FHW) was produced. The first (FHW1) consisted of quartz powder, fly ash and EP, while the second (FHW2) consisted of quartz powder, fly ash (FBC) and CBD. The reference (REF) contained only quartz powder (flour).

2.3.1. Composition of solidification products used

The proportions of individual components of the fillers for jointing grouts were chosen in connection with previous research [34] regarding the maximum possible use of hazardous waste while maintaining sufficient incorporation in the structure so that no pollutants are leached from the final products. A larger proportion of quartz powder has a positive effect on the chemical resistance of the final product. The ratio of the individual components of the solidified waste is given in Table 7, the structure of the filler can be seen from Fig. 6 and Fig. 7, the basic properties are noted in Table 8, the granulometry is presented in Fig. 8 and the ratio of the binder and filler components is shown in Fig. 9.

Table 7
Percental proportion of individual components.

Filler marking	**Filler Content [wt.%]**			
	Hazardous waste (HW)		Solidifying agents	
	End Product (EP)	Cement Bypass Dust (CBD)	Fly Ash (FBC)	Quartz Powder
FHW1	10	-	40	50
FHW2	-	10	40	50
REF	-	-	-	100

Fig. 6. Filler FHW1 (quartz powder, FBC, EP).

Fig. 7. Filler FHW2 (quartz powder, FBC, CBD).

Table 8

Properties of the fillers (solidified hazardous waste)

Parameter	Units	FHW1	FHW2	REF
Loose bulk density [kg/m^3]	[kg/m^3]	650	690	925
Tapped bulk density [kg/m^3]	[kg/m^3]	895	930	1140
Residue on sieve 0.2 mm	[%]	1.02	2.67	0.10
Water absorption	[%]	58.3	65.8	32.5

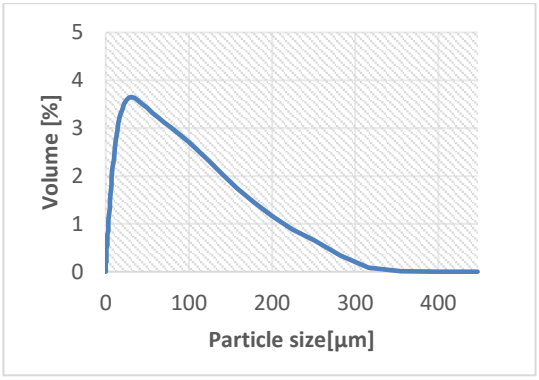

(a)

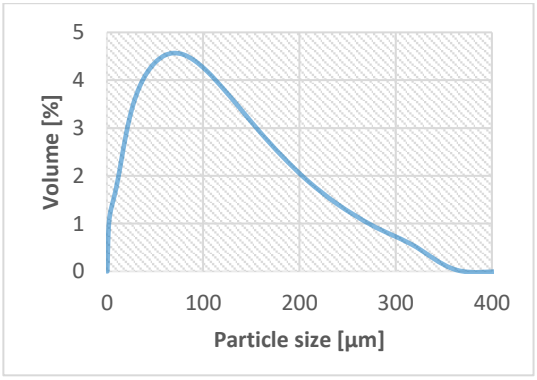

(b)

Fig. 8. Particle size distribution of the fillers: (a) FHW1; (b) FHW2.

2.4. Verified mixed design

Good mechanical properties and polymer composites' excellent chemical resistance make them cost-effective building materials for civil engineering applications, such as jointing grouts. Polymer grout properties depend on the type of polymeric binder and the filler materials used [35]. The effectiveness of by-products like fly ash in polymer mortars is well-known, mainly in the improvement of mechanical properties and reduction in water absorption [36]. The mix design for the polymer grout systems (Fig. 9) is optimised for workability, strength, durability, economy and environmental aspects depending on the intended application. The grout's formulation in mass per unitary volume (kg/m^3) is presented in Table 9. The specification of the resins and the curing agents can be seen in Tables 1-3.

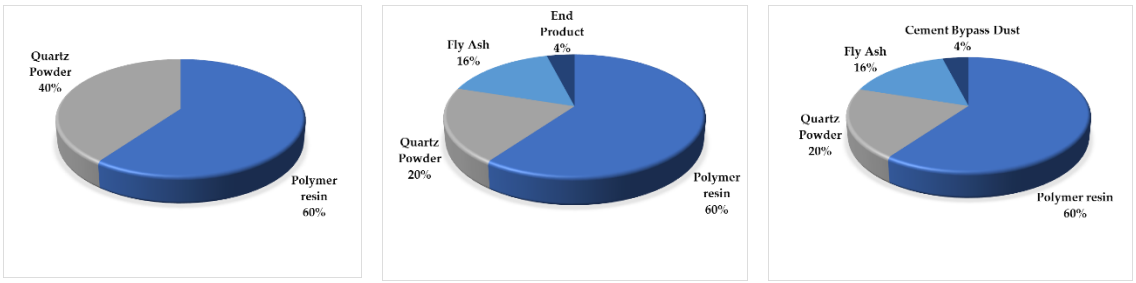

(a) (b) (c)

Fig. 9. Formulations of the jointing grouts: (a) Reference; (b), (c) containing solidification products. 3 types of polymer resin were used (HRG-D, ERG-D, MRG-W).

Table 9

Formulations of the polymer grouts in kg/m^3

Polymer grout	Filler	Epoxy resin	Curing agent	Quartz powder	Fly ash (FBC)	EP	CBD
	FHW1	527.8	213.4	536	459.5	93.6	-
ERG-D	FHW2	527.8	213.4	536	459.5	-	111.6
	REF	527.8	213.4	1072	-	-	-
	FHW1	517.2	235.4	536	459.5	93.6	-
HRG-D	FHW2	517.2	235.4	536	459.5	-	111.6
	REF	517.2	235.4	1072	-	-	-
	FHW1	476.3	252.0	536	459.5	93.6	-
MRG-W	FHW2	476.3	252.0	536	459.5	-	111.6
	REF	476.3	252.0	1076	-	-	-

3. Research Methods

All developed grouts were tested both under inert laboratory conditions and after degradation of chemically aggressive substances. Subsequently, changes in the most important properties of jointing grouts after the action of a chemically aggressive environment (hardness, compressive and flexural strength, abrasion resistance) were monitored. Among other things, the temperature resistance of jointing grouts not exposed to a chemically aggressive environment was also monitored to determine the maximum usable temperature of the developed jointing grouts in practice. A rheology of the grouts in the fresh state was observed by the dynamic viscosity. In the final phase, an advanced chemical resistance test was performed as part of pilot plant verification of selected jointing grouts.

3.1. Chemically aggressive environment

A harsh environment is often a combination of corrosive media, high temperature and fluctuating conditions. The corrosive media diffusion behaviour and the level of the physical and mechanical degradation of the specimens aged in that environment can differ depending on the concentration and type of aggressive media [37]. The chemically aggressive environments used were chosen with regard to the concentrations of aggressive media, which occur in real conditions of sewers or chemical plants, where cladding elements are used (e.g. from cast basalt) and it is necessary to ensure quality grouting with defined long-term resistance to chemical stress. The individual types and concentrations of the solutions used in the research are listed in Table 10 and Table 11. The samples were also immersed in simulated wastewater (WW). At the same time, in the first week, the desiccator was opened to bind

the bacteria to the solution, and subsequently, the closed desiccator with immersed samples was stored at 65 °C for 28 days.

Table 10

Selected chemical agents to which the grout samples were exposed.

Chemical substance	Mass concentration [%]	Temperature [°C]	Form of action	Duration of exposition [days]
H_2SO_4	96	60	acid vapours	28
	60	23	solution	
CH_3COOH	10			
HF	20	23		28
WW [1]	*	23; 65		28

[1] solution simulating WW* [38].

Table 11

Chemical composition of WW and individual concentrations of WW components.

	Casein	$NaHCO_3$	CH_4N_2O	NaCl	$CaCl_2$	$MgSO_4$
c [$g \cdot l^{-1}$]	1.90	5.30	4.60	1.10	0.53	0.17

3.2. Hardness

Hardness was determined by a specially designed procedure for samples of jointing grouts with dimensions of 70 × 70 mm and thickness of at least 30 mm. This procedure involved the use of a special steel cone (Fig. 10a) with a base of 20 mm, a height of 40 mm and a 2 mm concavely ground tip for better reproducibility of the hardness results of the grouts. The barrel steel used for its production was marked 34CRNIMO6Q. The test cone was fixed to the press and subsequently pressed into the sample at a speed of 5 mm/min (Fig. 10b). When the cone was pressed into the sample to a depth of 2 mm, the force was stopped and the maximum pushing force was subtracted.

(a)

(b)

Fig. 10. Principle of hardness determination: a) used cone, b) pushing of the cone during hardness determination.

3.3. Abrasion resistance

Abrasion resistance was determined according to EN 13892-3 [39] for samples of jointing grouts with dimensions of 70 × 70 mm and thickness of at least 30 mm, as was the case for the hardness test.

3.4. Compressive and flexural strength

Compressive and flexural strength were determined in accordance with EN 12808-3 [40], for test specimens in the shape of prisms with dimensions of 20 × 20 × 100 mm. Fresh grouts, after preparation, were cast into silicone moulds, where the samples polymerised (curing at 23 °C). After 24 hours, the samples were demoulded and stored in a laboratory environment. Subsequently, after 14 days, the prisms were placed into the desiccators with different aggressive environment represented by the solutions listed in Table 10. Sealable laboratory desiccators with a porcelain plate were used because of their highly chemically resistant borosilicate glass with long-term temperature resistance up to + 70 °C. After the desiccators were sealed, and the samples were stressed by the aggressive environment for 28 days. After removal from the desiccators, the samples were rinsed and dried under laboratory conditions. Samples stressed by a chemically aggressive environment were also visually evaluated before the test itself in regard to colour change, cracking and segregation of the filler and surface layers of jointing grouts due to the aggressive environment.

3.5. Glass transition temperature

The glass transition temperature (T_g) determination, which can represent a way to assess the maximum usage temperature of the polymer grouts, was performed using dynamic mechanical analysis (DMA). T_g represents the limit temperature at which the polymer can withstand the required stress, even the system may not be degraded. The measurements were performed in the temperature range of 40–130 °C at a heating rate of 5 °C/min, an amplitude of 10 µm and a frequency of 1 Hz. The sample dimensions were 35 (active 17.6) × 3.3 × 12.0 mm, with two samples measured from each material.

3.6. Dynamic viscosity

The dynamic viscosity was determined to compare the fresh grouts' rheology, depending on the resin. After mixing all the components with a rotary viscometer, type Elcometer 2300, the grouts' dynamic viscosity was immediately determined. At the beginning of the viscosity determination, the mixture's temperature was 22 °C.

3.7. Study of microstructure

Using a Keyence VHX950F digital optical microscope, changes in the microstructure of jointing grouts – caused by the action of chemically aggressive substances – were monitored. Furthermore, the connection of the jointing grouts to the base (molten basalt), any occurrences of pores in the structure, microfractures, microcracks and microblisters were observed. Using an optical microscope, the method of breaking the surface of jointing grouts after the chemical resistance test and after the hardness test was also monitored in regard to the degree of indentation of the tip in the material and the detection of the degree of inert damage. The degree of penetration of aggressive solutions into the internal structure of the jointing grout and the influence of the aggressive environment on the degradation of the used polymeric binder and solidification product as filler were monitored.

The scanning electron microscope (SEM), TESCAN MIRA3 XMU, was used to explain the bonding effects of polymer resins with the filler. SEM was also used to evaluate the impact of aggressive media on the microstructure of the grouts. X-ray powder diffraction (XRD) analysis was used to reveal new crystalline structures that may have been formed by the reaction of the filler particles with aggressive solutions – acids. After chemical stress for XRD analysis, the samples were ground and sieved through a 0.063 mm mesh.

3.8. Advanced chemical resistance monitoring

Chemical resistance monitoring was performed as part of pilot plant verification for samples that met the basic requirements to simulate real chemical stress acting on the developed jointing grouts. Grouts with the ERG-D and HRG-D binders were examined. Cast basalt tiles (20 x 20 cm, thickness of 22 mm) were jointed and anchored to a cohesive base (cement-bonded particleboard) using polymer cement adhesive. The tiles were grouted after 14 days. The basalt elements used are typically utilised in the most demanding industrial plants and conditions, including sewers; thus, a large-format sample with real joints was created. Jointed surfaces with a thickness of 4–5 mm were evenly exposed to the proposed aggressive agents (see Fig. 11). Aggressive solutions (60% H_2SO_4, 10% CH_3COOH, 10% HCl, 10% HF) were applied on the surface at checkpoints bounded by a closed 90 mm diameter polyethylene terephthalate vessel that had no bottom and was fixed to the surface with sanitary silicone, the level of the aggressive solution was 20 mm from the test surface. After a test period of 28 days, the samples were cut with a diamond blade saw, and properties such as adhesion to basalt, hardness and microstructure (degree of penetration of the aggressive medium into the examined jointing grout, method of surface failure and microdefects) were monitored.

(a) (b)

Fig. 11. Samples prepared for pilot plant verification of properties: (a) prepared base, (b) samples exposed to aggressive agents.

4. Results and discussion

4.1. Visual assessment of chemical resistance

There was no visual change in the HRG-D-based grout due to the action of 96% sulphuric acid vapours. As a result of the direct action of the 60% sulphuric acid solution, the colour brightened and turned red (Fig. 12a). Due to the action of 10% acetic acid solution (CH_3COOH), a colour change occurred; in addition, colour spots formed on the surface (Fig. 12b). The acid corrosivities are dependent on the chemical reactions running between the acid and the epoxy resin chain; these chemical reactions ran in parallel with purely physical diffusion processes [41]. The poor resistance of epoxy resins to organic acids occurs because of the unreacted amine curing agents or water trapped inside the grout. An

inhomogeneous film structure, due to insufficient coalescence during the curing process, also leads to poor resistance [42]. Generally, room temperature-cured epoxy resins have poor resistance to organic acids. However, at lower concentrations, the resistance is much improved [43]. The oxidation degradation of epoxy-based materials only occurs within the surface layer, effectively reducing oxygen diffusion and finally reaching a limited thickness to protect the inner cores from further oxidation. High temperatures can catalyse the formation of the oxidised layer [44]. Oxidation and hydrolysis can occur after the ageing of polymer grouts and are irreversible [45]. For the reference sample filled with quartz flour, no spots formed, but a colour change occurred. However, no colour changes resulting from the effect of the simulated WW transpired. From the point of view of visual assessment, FHW2 appears to be the most suitable filler out of those examined. A 30% acetic acid solution led to significant degradation and total decomposition of all samples (Fig. 12c). The action of a 10% acetic acid solution on the water-compatible MRG-W jointing grout resulted in the total decomposition of the structure only in the reference sample with quartz flour (Fig. 12d). The decomposition of the sample was caused by the Fe_2O_3 content of the pigment, which reacted with acetic acid according to the following equation:

$$Fe_2O_3 + 6CH_3COOH \rightarrow 2(CH_3COO)_3Fe + 3H_2O \quad (4)$$

(a) (b) (c) (d)

Fig. 12. Grout samples after exposition to chemical aggressive media: a) samples ERG-D after exposition to 60% H_2SO_4 (grooves are after strength tests); b) samples ERG-D after exposition to 10% CH_3COOH, (c) samples ERG-D after exposition to 30% CH_3COOH, (d) sample MRG-W after exposition to 10% CH_3COOH.

4.2. Hardness

A graphical evaluation of the results of the hardness testing is presented in Fig. 13. In the lower part of the graph, the percentage changes in hardness due to aggressive environment are shown in comparison with reference samples stored only in a laboratory environment. Samples with the HRG-D and MRG-W binders increased their hardness when exposed to a sulphuric acid solution (this could be due to the formation of sulphate neoplasms that filled the pores of the grout). Compared to the reference filler, the samples with the newly formed solidification products (FHW1 and FHW2) achieved higher hardness due to the higher degree of hardness of the filler component. Due to the more suitable shape index of the particles, a better homogenisation of the mixture and, therefore, better incorporation of the filler component in the polymer matrix was possible. It can be observed that the action of both vapours and sulphuric acid solution increased the surface hardness of most grouts. This is likely caused by the reacted surface layer, which filled the surface pores and thus increased the surface hardness; this layer was evident in visual evaluation. When the epoxy specimen is dried completely and reach a mass stabilization, a little amount of acid solution still remains in the specimen

[46]. For the sample with the reference binder exposed to acetic acid, the structure was completely decomposed, and the hardness could not be determined at all. Surface hardness is important for jointing grouts in chemically aggressive environments, as it can be concluded from higher hardness values that the material will withstand mechanical stress when mechanical resistance is high. Hardness, as well as abrasion resistance (especially in the lower part of the profile, see below 4.3), is especially important for jointing grouts in sewer environments (which must withstand mechanical cleaning, scrapers, water jets, damage caused by an introduced foreign sharp element, etc.) and ensures they will not be damaged. It was showed by Zhang et al. [47] that hardness depends not only on the degree of cure but also on the thermal history during curing process. Fillers that increase the elastic modulus of epoxy composites increase the hardness of the composite – hardness is a function of the relative filler or fibre volume and modulus [48].

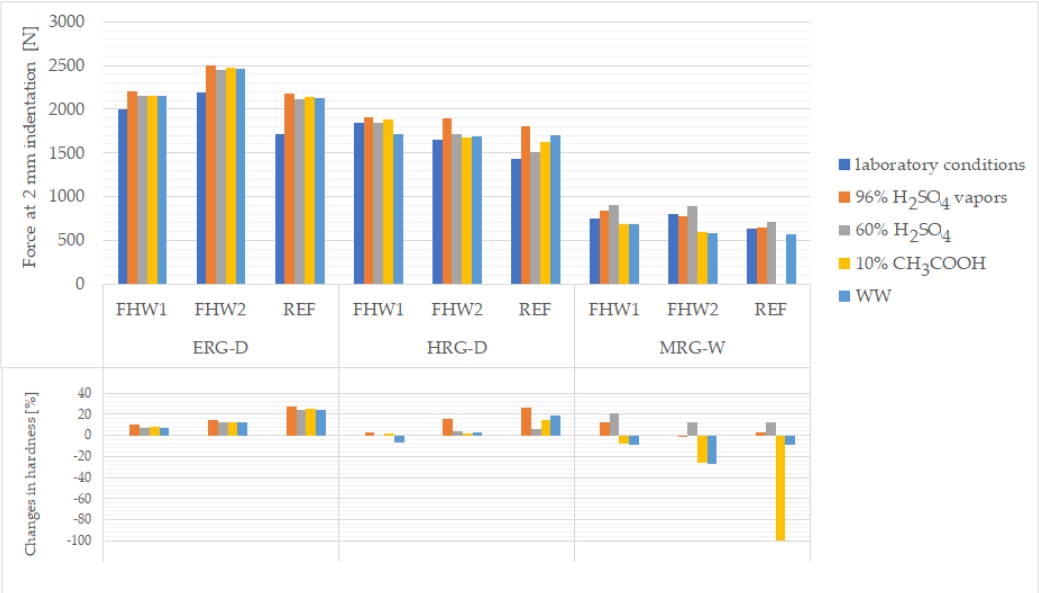

Fig. 13. Evaluation of the influence of a chemically aggressive environment on the surface hardness of jointing grouts.

4.3. Abrasion resistance

Abrasion resistance was determined before and after exposure to a chemically aggressive environment. The results of the determination of abrasion resistance show that the abrasion resistance deteriorated due to the action of a chemically aggressive environment. From Fig. 14, it can be seen that the greatest deterioration in abrasion resistance occurred in the HRG-D samples using the reference quartz flour filler. The MRG-W sample with the reference filler was completely degraded in the CH_3COOH solution as described above, so the abrasion resistance could not be determined at all. The results of all samples show that the exposure of the grouts to chemically aggressive environments led to the deterioration of abrasion resistance. This is caused by the degradation of surface layers due to surface damage, which became less resistant to abrasive stress; thus, there was greater volume loss for the grouts.

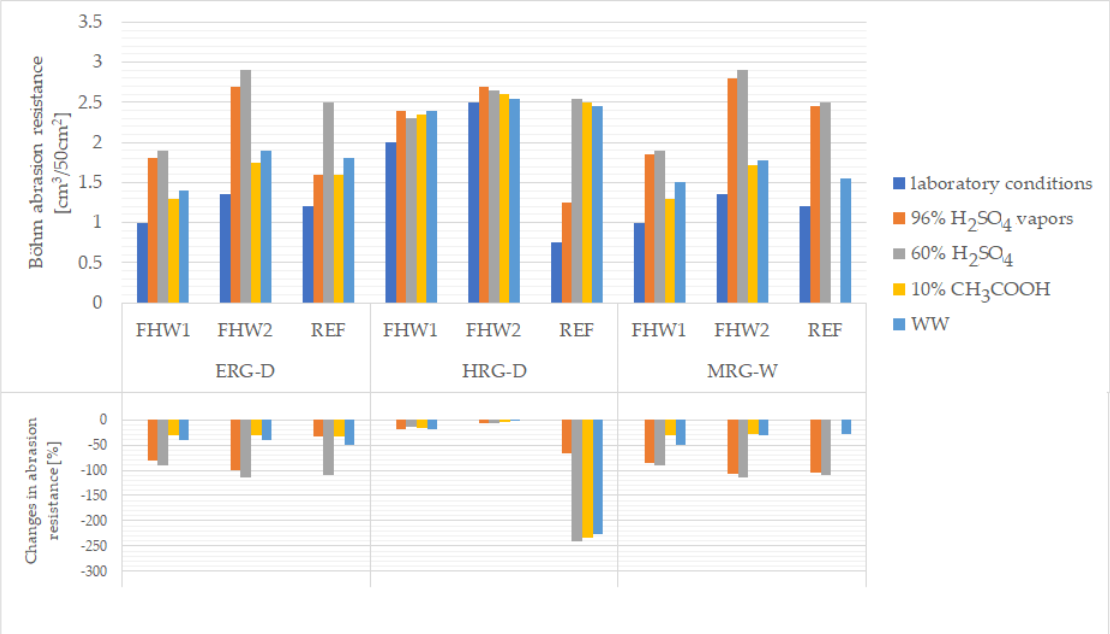

Fig. 14. Evaluation of the influence of a chemically aggressive environment on the abrasion resistance of jointing grouts.

4.4. Flexural and compressive strength

Due to the direct action of the 60% solution and the vapours of the 96% sulphuric acid solution, the three-point flexural strength increased in all samples (the most significant increase was recorded for grouts with highly chemically resistant epoxy resin ERG-D). The grouts with the ERG-D and HRG-D binders achieved strengths comparable to the reference filler when using solidification products as filler (Fig. 15 and Fig. 16). The CH_3COOH solution had a negative effect on the flexural strength of all samples examined. The excellent parameters of epoxy adhesives may be modified by the environment which often acts as a degrading agent [49]. The effect of sulphuric acid on epoxy resin composites was also researched by Ribeiro et al. [50], who found that the flexural strength of epoxy polymer concrete was only slightly affected by immersion in this solution, indicating good chemical resistance to this type of aggressive environment. Mebarkia et al. [51] found that after one-month immersion in chemical solutions with different pH levels, the flexural and compressive strength of polymer concrete decreased with higher pH levels. The affecting of flexural strength and modulus due to ageing was showed in the previous study [52], where both properties had an initial, steeper decay and tended to stabilise later.

Epoxy is inherently brittle, and it has a low fracture toughness [37]. The load-deflection diagram from the bending test is presented in Fig. 17 and the compressive strength test in Fig. 18. A depression to the deflection of 0.5 mm was noted for all samples, except the sample MRG-W_REF. Region of reduced tangent stiffness was recorded only with MRG-W grouts. The ultimate strength of ERG-D and HRG-D specimens was recorded at the end of the linear part of the curve. Under compressive stress, the loading of ERG-D and HRG-D samples were linear until the failure. For MRG-W samples, nonlinearity was recorded in the area of maximum strength. Subsequently, the deformation increased, while the force decreased until the sample's failure, in this case, the maximum strength, did not correspond to the sample's failure. It is also evident from the diagrams that the MRG-W jointing compound showed a lower modulus of elasticity. The stress concentration plays a major role

in the type of fracture. It may overshadow the strain rate effect on modulus of rupture in flexure, the degree of nonlinearity, and the epoxy grout's overall response [53]. The elastic modulus and tensile strength of epoxy-based adhesives decrease with the number of ageing cycles [54]. Previously, the epoxy systems were exposed to 50 °C for 28 days, and this exposure led to a 15% increase of T_g, and the flexural strength increased 32% due to the density increase of crosslinking [55]. Due to the direct action of the 60% sulphuric acid solution, the compressive strength of the samples ERG-D and HRG-D increased (the most significant increase occurred in the grouts with highly chemically resistant epoxy resin ERG-D with a reference filler made of quartz flour). This increase, noticeable form Fig. 16, is due to the formation of small crystalline neoplasms in the porous structure resulting from the direct action of H_2SO_4 on silicate compounds, which filled the pores and thus created a more compact structure. The negative effect of 10% acetic acid solution on compressive strength was not demonstrated. In the samples with the MRG-W resin used with the reference filler, the structure was completely decomposed due to the action of CH_3COOH (see Fig. 12d).

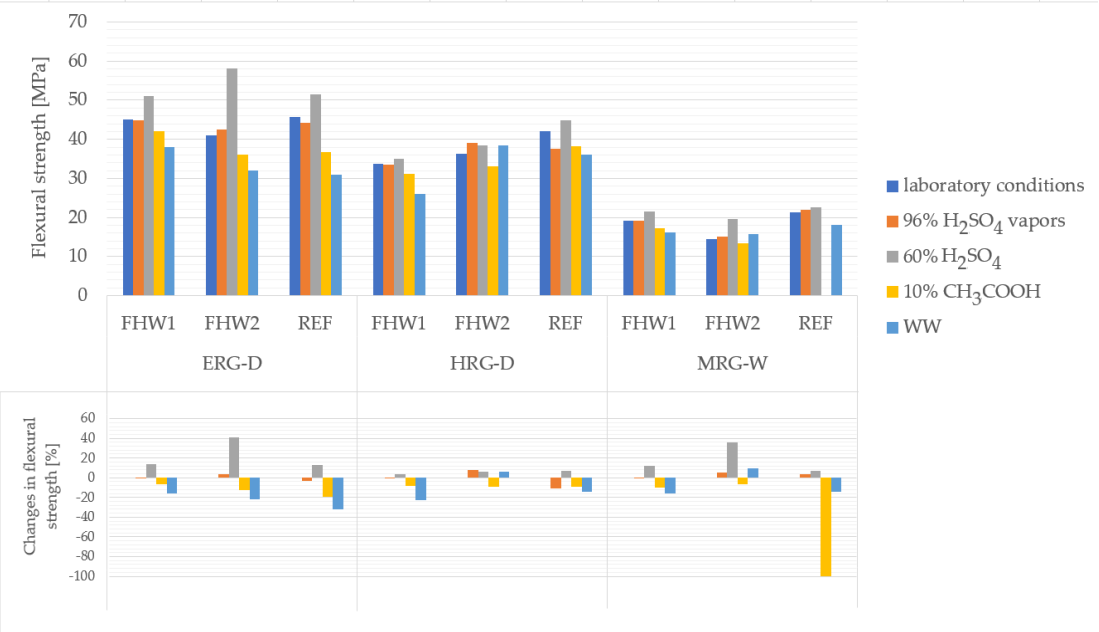

Fig. 15. Evaluation of the influence of a chemically aggressive environment on the flexural strength of jointing grouts.

Fig. 16. Evaluation of the influence of a chemically aggressive environment on the compressive strength of jointing grouts.

1

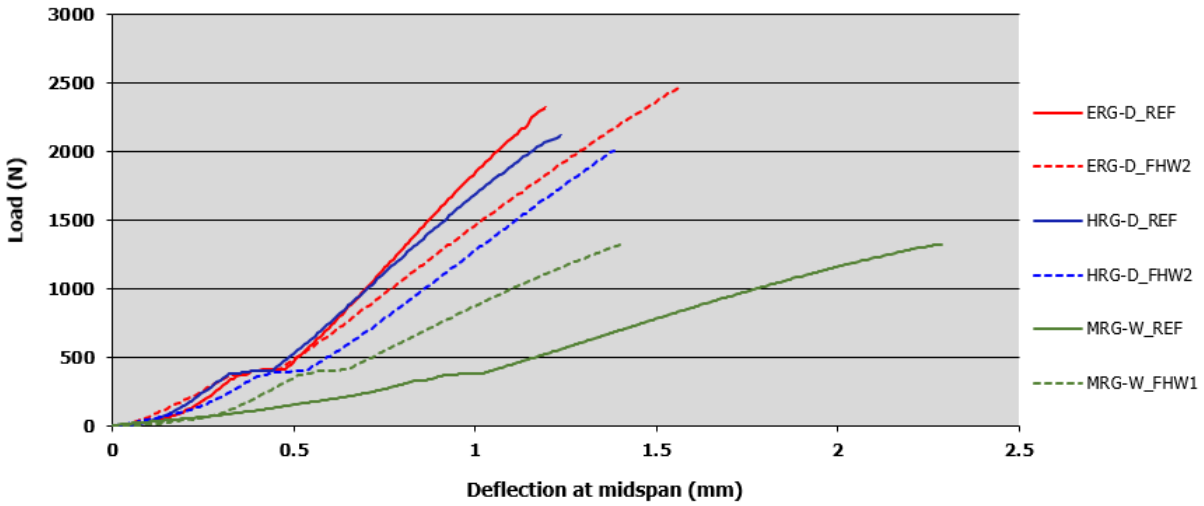

2

3 **Fig. 17.** Load-deflection diagram from the bending test.

4

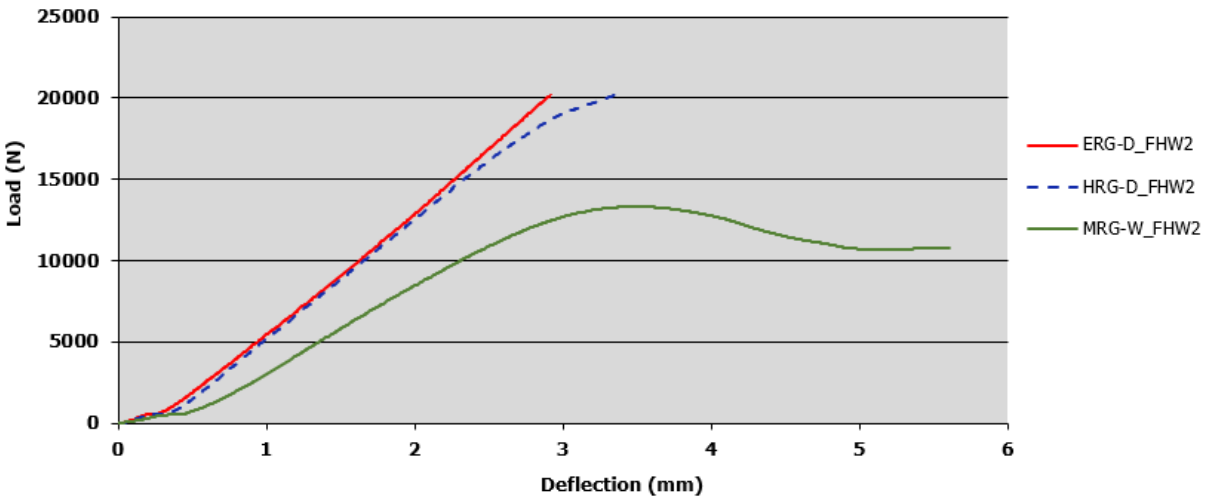

Fig. 18. Load-deflection diagram from the compressive strength test.

4.5. Glass transition temperature

As can be seen from Fig. 19, it is clear that the type of filler used does not have a significant effect on the glass transition temperature (T_g). Only the type of resin used has a fundamental influence. The highest T_g values (approx. 70 °C) were reached by the water-compatible epoxy resin MRG-W, while the lowest values were reached by the chemically resistant resin HRG-D (approx. 60 °C). As HRG-D grouts can withstand temperatures of 60 °C, their use in sewers and chemical plants is therefore possible. Lesser et al. [56] stated that reactions of epoxide groups with primary and secondary amines are more favoured than the base catalysed epoxide etherification reaction.

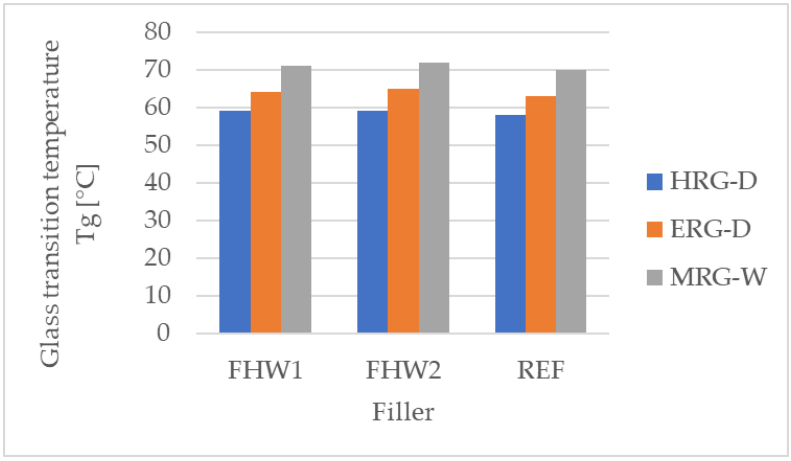

Fig. 19. Glass transition temperature.

4.6. Dynamic viscosity

The results of dynamic viscosity are presented in Fig. 20. The highest value of the viscosity (149,000 mPa·s) was achieved with the mixture ERG-D containing a 40% solidification product FHW2 as the filler. ERG-D resin also exhibited the highest viscosity of the three used. The reference grouts, in which the quartz flour was used, showed the lowest viscosity due to the particle size, the specific surface area,

and the filler's shape index. The type of solidification products (FHW1, FHW2) did not significantly affect the mixture's viscosity. It can also be seen from the results that the epoxy resins used influenced the viscosities of the jointing grouts, the highest being achieved with ERG-D binder. The polymer binders' viscosity is determined primarily by their composition (type of ER, type and number of solvents, hardeners, and other additives). The rheology of epoxy resins was also investigated [57],[58], providing information on viscosity changes along with the curing process. During the ER curing, the molecular size increases, as does the crosslinking density, decreasing mobility and increasing the resin system's viscosity [58].

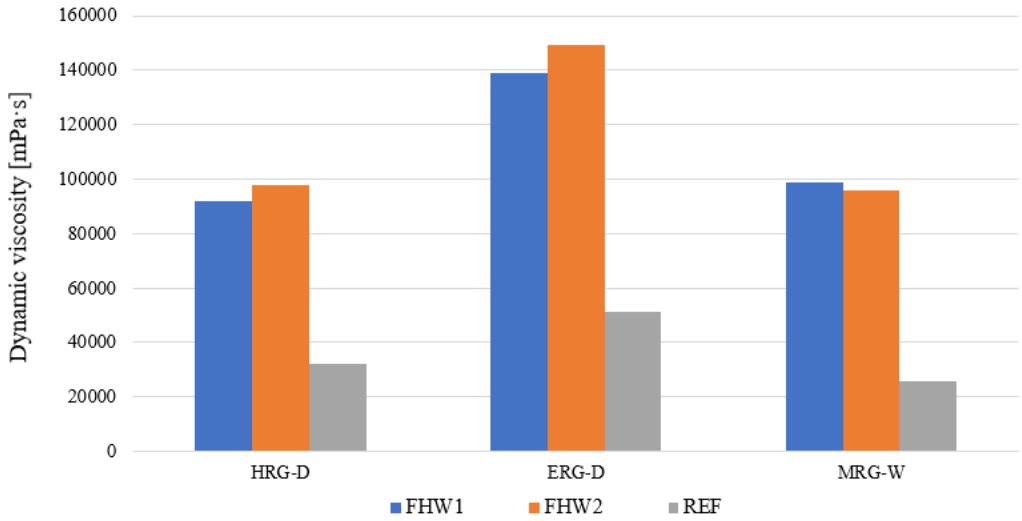

Fig. 20. Dynamic viscosity of the fresh polymer grouts

4.7. Study of microstructure

In the hardness test, the sample was loaded until the test tip of the cone was pressed into a depth of 2 mm. Subsequently, the created indentation was examined microscopically. By observing the microstructure after pilot plant verification of the properties, it was proven that even with the action of aggressive substances, there were no major changes compared to the reference sample. The indentation profile of the test cone in the surface sample after the chemical resistance test in the 3D model can be observed in Fig. 21 and Fig. 22. Regarding the evaluation of the acquired images, it can be stated that the type of filler also influenced the shape of the indentation of the pressed cone in the jointing grout. The type of aggressive medium also had an effect on the way the cone penetrated the surface of the grout. The effect of the microstructure on the diffusion rate depends on the type of epoxy composite: the type of epoxy resin and hardener, the epoxy to hardener ratio, and the type of filler [59],[60].

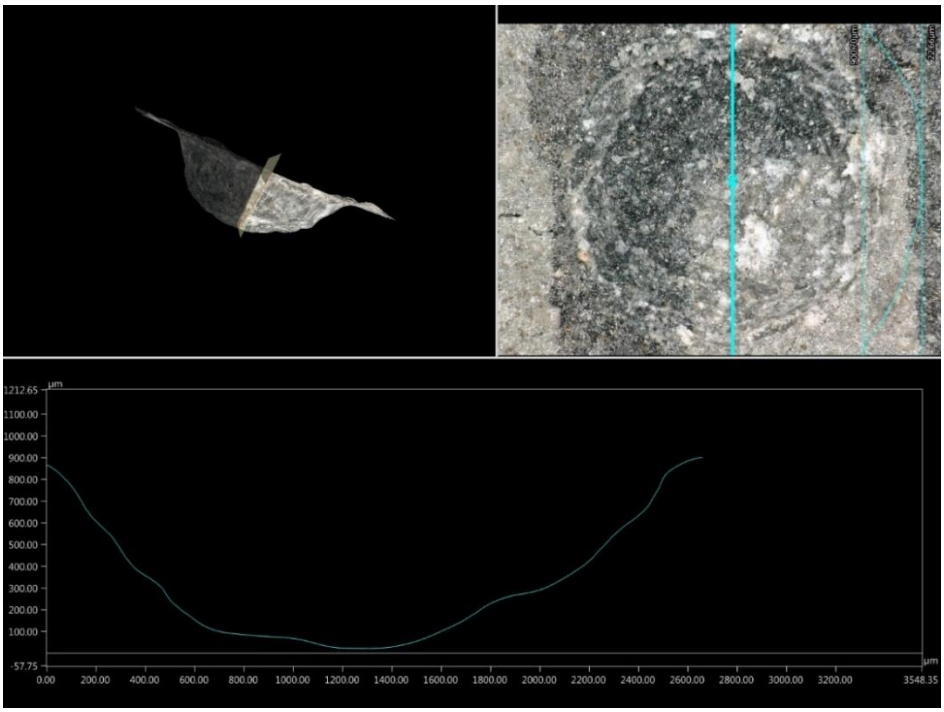

Fig. 21. Indentation profile of the test cone to the HRG-D REF sample surface after the chemical resistance test due to the action of CH_3COOH in the 3D model.

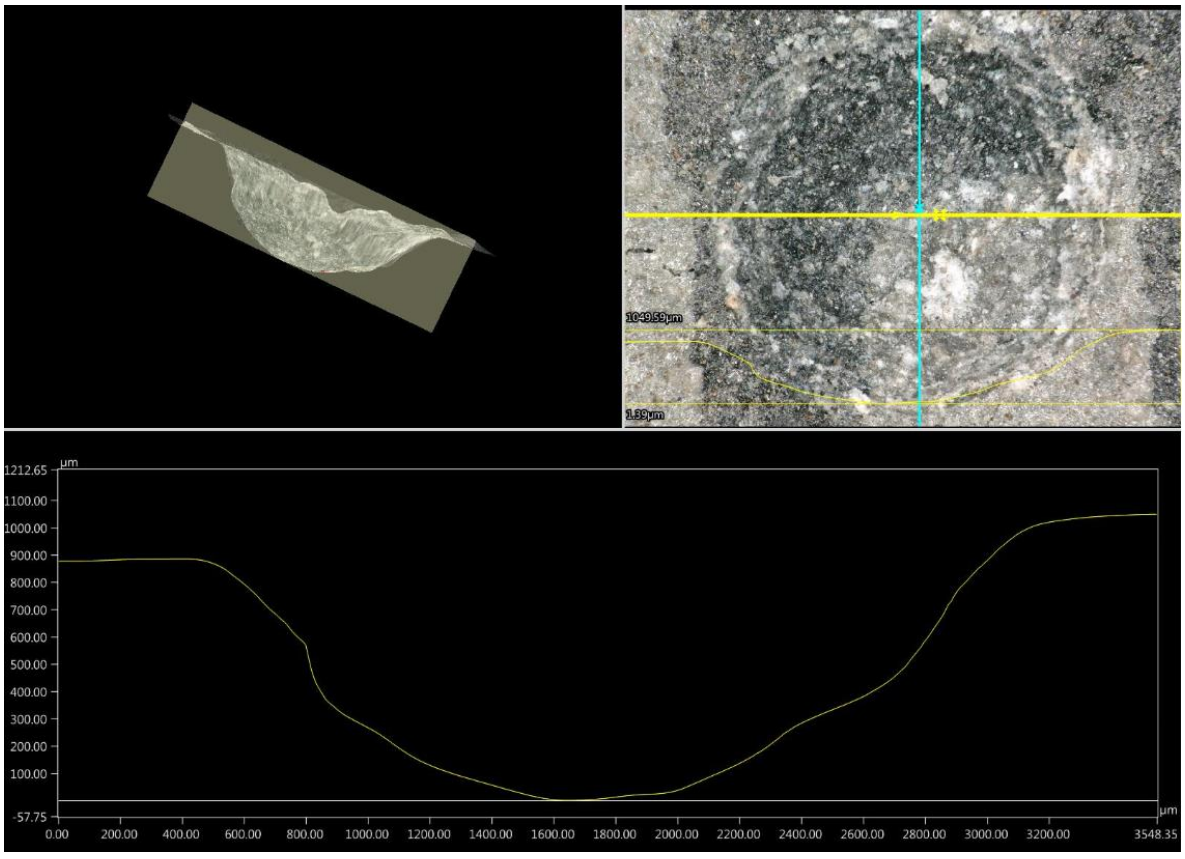

Fig. 22. Indentation profile of the test cone to the HRG-D FHW2 sample surface after the chemical resistance test due to the action of CH_3COOH in the 3D model.

The diameters of the indentation passing through the centre of the interleaved circle were measured (Fig. 23). The picture also shows the method of failure near the indentation, around which small cracks

formed, which could be a source of further propagation of defects in the future due to the cyclic mechanical stress of the grout.

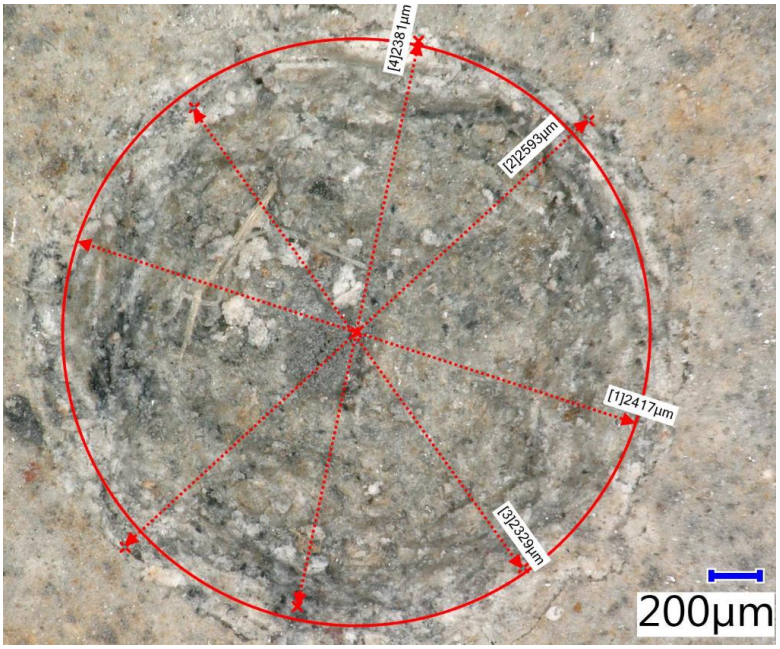

Fig. 23. Measurement of test cone indentation diameters (HRG-D FHW2) after H_2SO_4 immersion.

Fig. 24 shows the diameters and surface areas of indentation of the test tip into the surface of the test sample for surface hardness determination after pilot plant verification in a chemically aggressive environment. When the samples with the ERG-D resin were exposed to sulphuric acid and acetic acid, the diameter of the test cone indentation increased for all types of fillers used in this test. Samples with the HRG-D binder and reference filler behaved similarly. The FHW2 filler used in combination with the HRG-D binder caused the indentation to have a smaller diameter compared to the sample not exposed to aggressive media. Samples with the MRG-W binder, which were exposed to sulphuric acid, had a larger indentation diameter compared to the reference sample. The MRG-W FHW2 sample had a smaller indentation diameter compared to the reference sample. The sample with the reference binder, exposed to acetic acid, experienced total decomposition of the structure; thus, the hardness could not be determined at all.

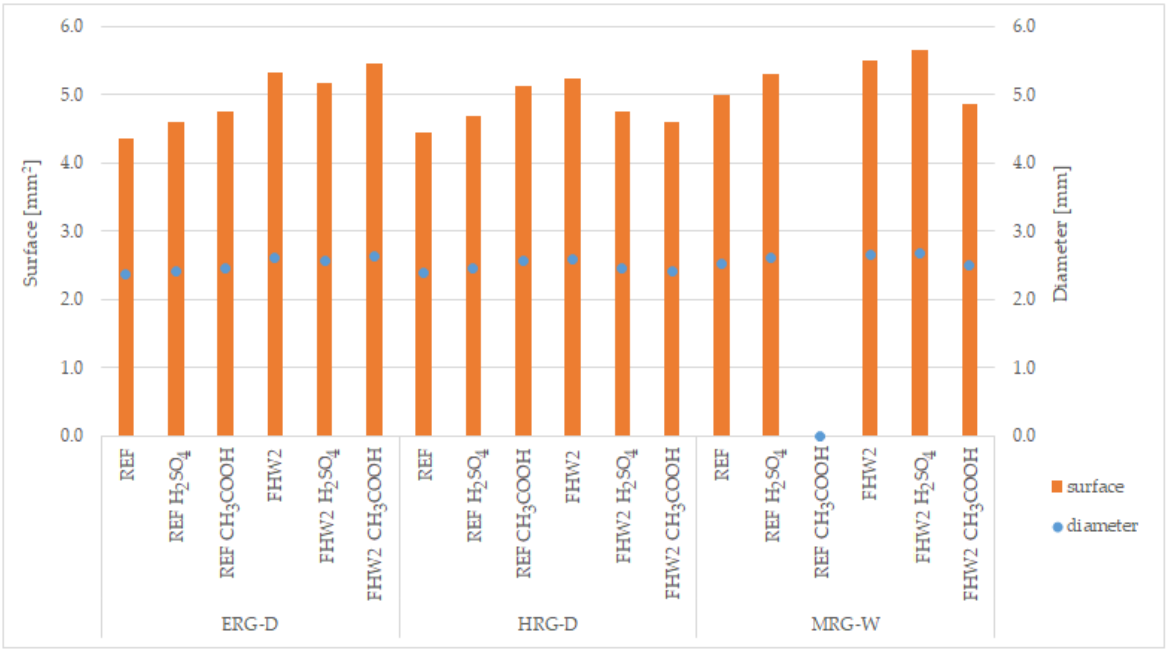

Fig. 24. Diameters and areas of the indentation of the test cone tip into the surface of the examined sample during the test of surface hardness determination – determined microscopically.

Fig. 25 shows the connection of the grout of the reference sample without chemical stress to the underlying cat basalt (darker part). A strong contact zone between the basalt and the grout was observed, with no larger air pores visible at the interface that could impair the cohesion between these materials.

(a) (b)

Fig. 25. The connection of the HRG-D grout to the cat basalt element: (a) magnification 6.4×; (b) magnification 16×.

With SEM analysis, the filler (solidification products) was found to be evenly dispersed in the polymer matrix. No clumps of filler or segregation were visible, and the contact zone between the filler and the polymer matrix was cohesive. Images (Fig. 26) show the crystals in the filler and neoplasms formed by acid and silicate-based filler's reaction. In Figures 26a and 26b, the grains of quartz flour, which increase the chemical resistance, are marked in yellow. The degree of penetration of hydrochloric acid into the grout's surface is shown with a red line. These images clearly show the unaffected and affected part of the grout with HCl. Fig. 26c shows pores in the grout whose size is between 10-80 µm. Some

pores closer to the stressed surface are partially filled with neoplasms. CaF_2 crystals formed by the reaction of the filler containing free CaO with hydrofluoric acid can be observed in Fig. 26d. The photomicrograph 26e shows acicular crystals (probably of aragonite) and the epoxy matrix disturbed by acetic acid. In Figure 26c, calcium acetate may be present, and the formation of irregularly shaped pores is evident. The microstructure of a sample stressed with sulfuric acid can be seen in Fig. 26f, the visible crystals representing both the particles of the filler in the polymer matrix and probably also the anhydrite formed by the reaction of the filler with sulfuric acid. Figure 27 (EDX spectrum of the grout exposed to 10% HF) confirms the presence of fluorine due to the penetration of HF into the sample while also showing the amount of Ca, so it can be concluded that the crystals practically correspond to CaF_2.

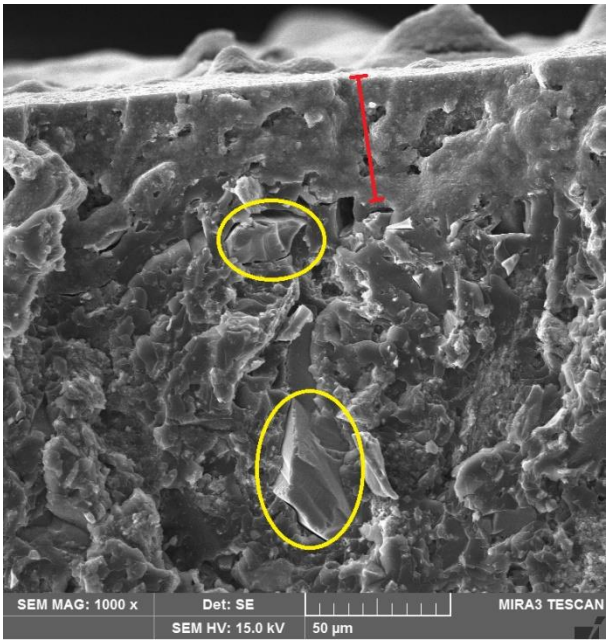

(a)

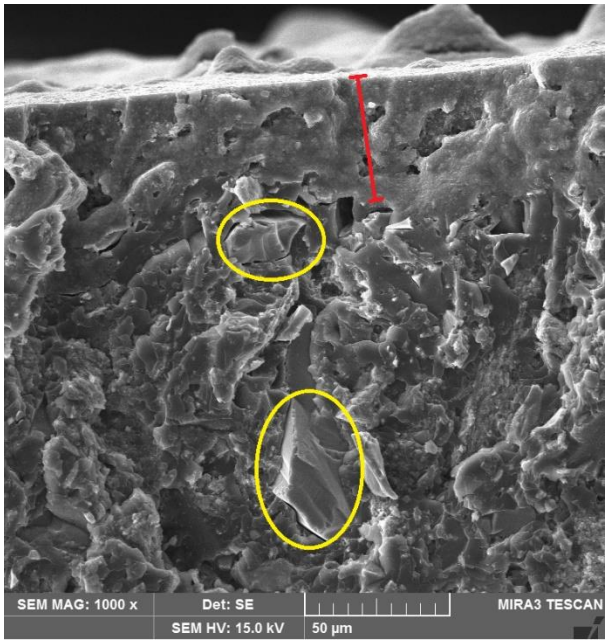

(b)

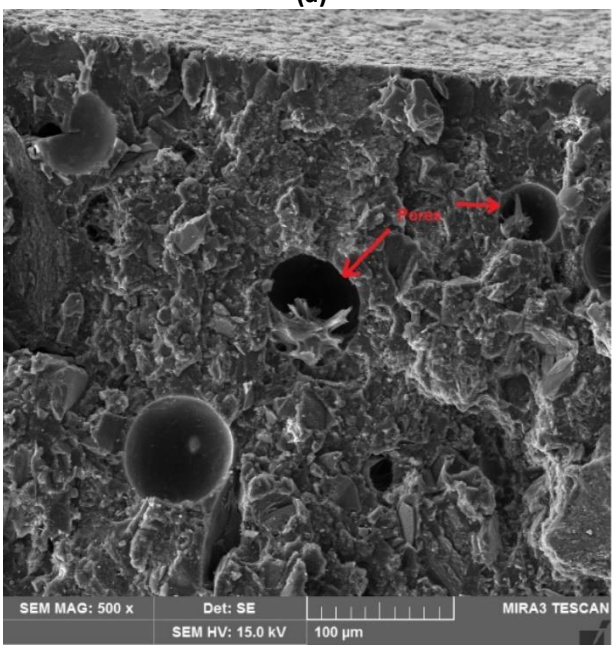

(c)

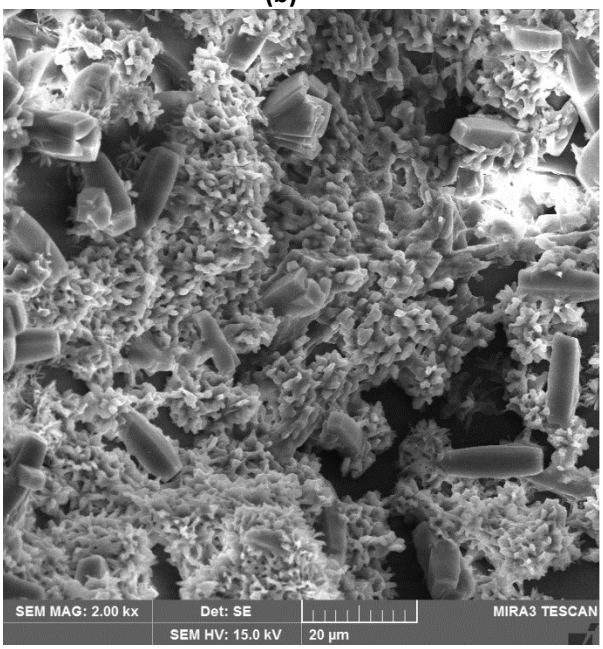

(d)

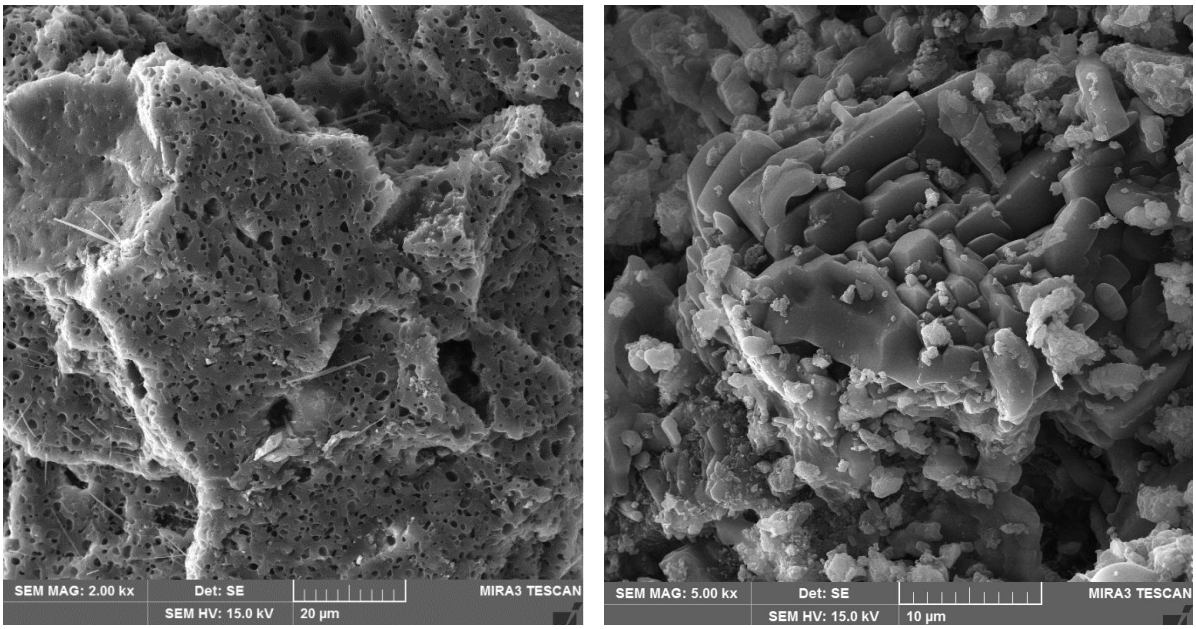

(e) **(f)**

Fig. 26. SEM micrographs of the grouts (fracture surface) after exposure to chemical aggressive media: a) HRG-D_FHW2 (10% HCl); b) ERG-D_FHW1 (10% HCl); (c) ERG-D_FHW1 (10% CH_3COOH), (d) HRG-D_FHW2 (10% HF); (e) ERG-D_FHW1 (30% CH_3COOH); (f) HRG-D_FHW2 (60% H_2SO_4).

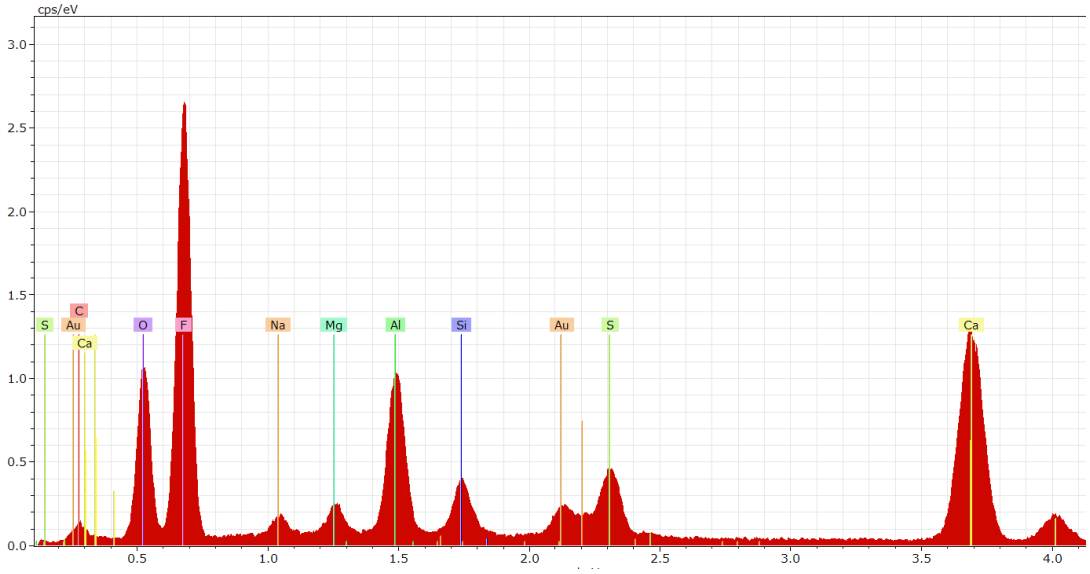

Fig. 27. Energy dispersive X-ray analysis (EDX) spectrum of the grout surface exposed to 10% HF.

Results of XRD analysis of the samples stressed by aggressive media in Fig. 28 did not confirm the formation of new crystalline neoplasms between aggressive media and the filler. No chemical reactions have occurred between the filler and the epoxy resin, and there were only physical connections between the filler particles and the epoxy matrix. XRD diffractograms present only minerals that were already found in the fillers (β-quartz, portlandite, calcite, anhydrite). The grouts' polymer matrix showed so much chemical resistance that it protected the filler particles with a perfect coating, which was also proved by the XRD pattern of samples subjected to chemically aggressive environments. It follows that aggressive solutions did not penetrate the structure of the jointing grouts too deeply.

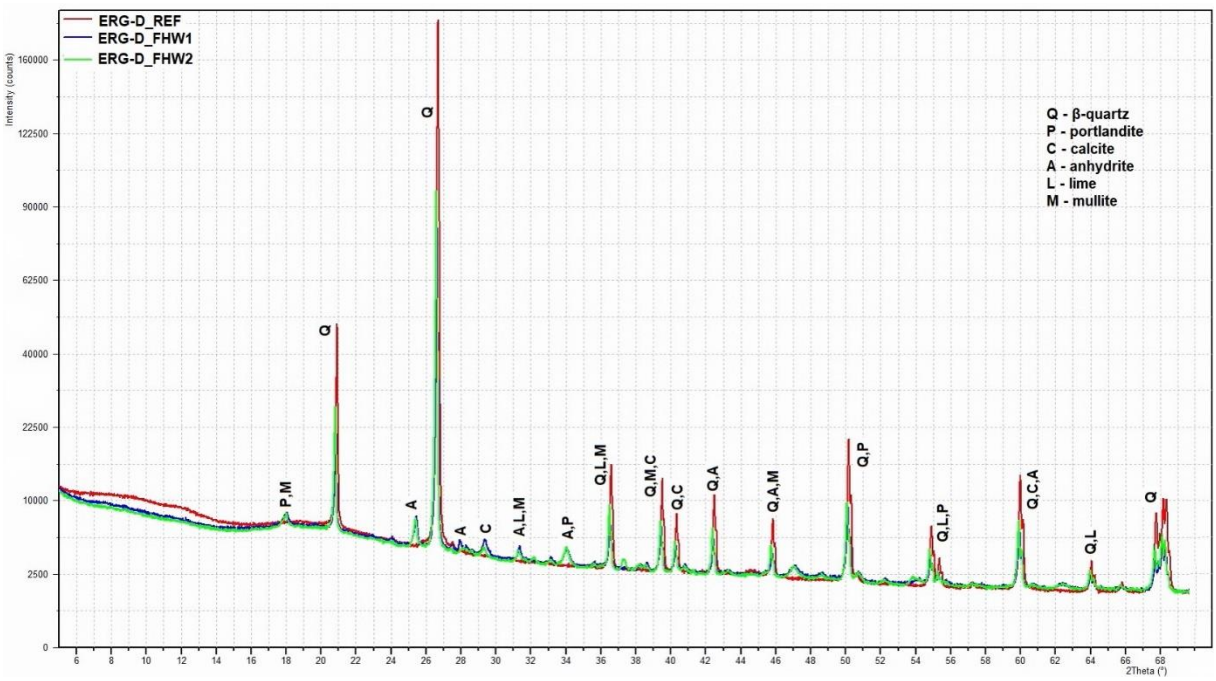

Fig. 28. X-ray diffraction pattern of the grouts after exposure to chemically aggressive media (only crystalline structures of the fillers were found).

Fig. 29 shows how the colour of the jointing grout was changed, and the deterioration of the surface is obvious by the action of hydrofluoric acid; the upper part of the figure experienced no disturbance (REF), whereas the lower part was exposed to chemical aggressive media Fig. 30 shows a method of separating the grout from the base after a hardness test, in which the adhesion of the grout to the molten basalt was impaired.

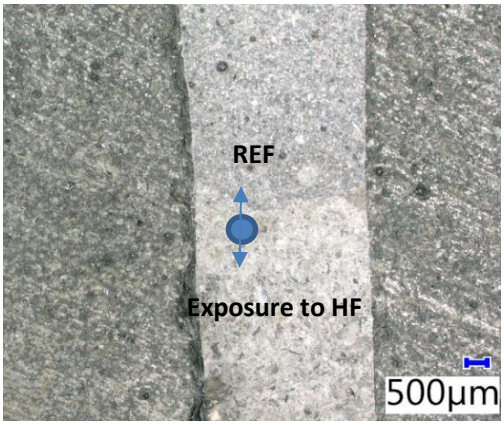

Fig. 29. ERG-D grout – transition of the zone without chemical stress (upper part) into the zone after the action of HF (lower part).

Fig. 30. Separation of ERG-D grout from cast basalt element after exposure to HCl.

Fig. 31 displays the transition of the grout which was affected by the aggressive environment at the impression site. In Fig. 32, the gradual effect of acetic acid can be observed on the surface; the left shows the unexposed sample, while the right shows the front surface after being directly exposed to 10% acetic acid solution. Loh et al. [61] showed that the diffusion parameters and aggressive media

uptake are affected by the relative humidity (R.H.), temperature of the environment, the epoxy microstructure, and the thickness of the material.

Fig. 31. HRG-D grout – transverse view of grout interface (REF/HCl) at the indentation site.

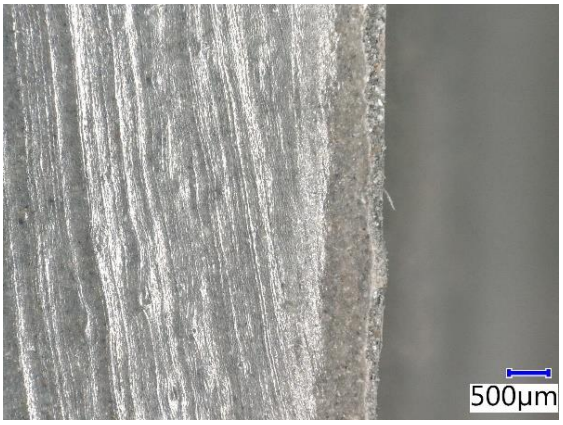

Fig. 32. HRG-D grout – transverse view of the transition from the greater depth of the joint (left) to the outer surface of the grout (right) – reacted, after the action of CH_3COOH.

The results for the hardness determination after pilot plant verification are shown in Fig. 33. Samples with the ERG-D binder used achieved higher values for the force required to engage the tip of the test cone and thus achieved greater hardness compared to HRG-D samples. Acetic acid severely disrupted the HRG-D sample, which also resulted in a decrease in surface hardness.

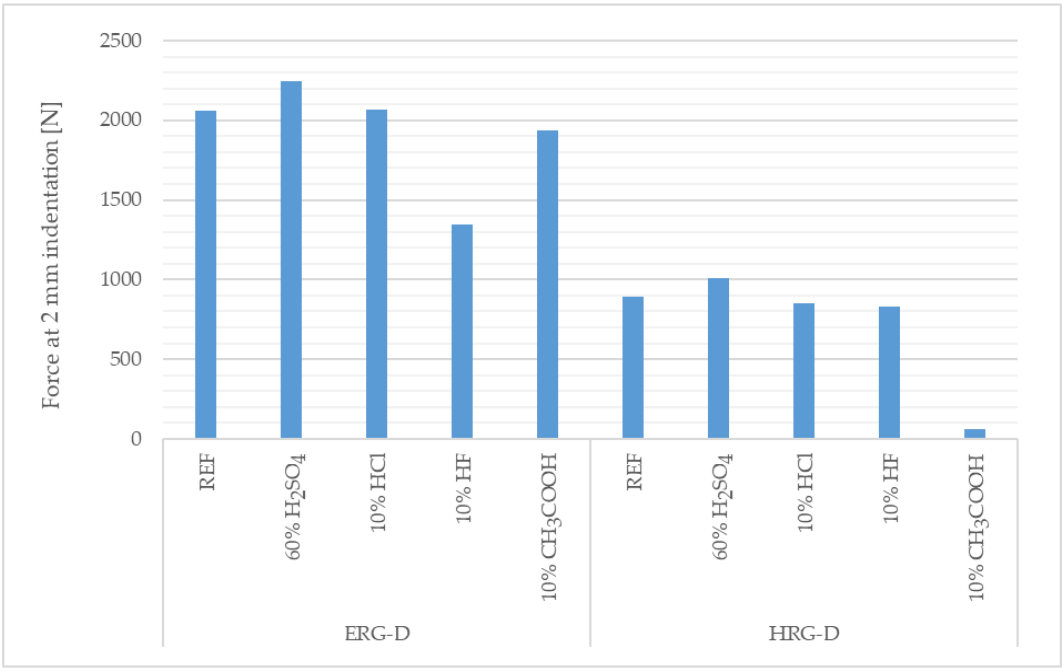

Fig. 33. Force at the 2 mm indentation after pilot plant verification.

5. Conclusions

Based on the new progressive methodology of chemical resistance testing, the most important properties of the newly developed polymer chemically resistant jointing grouts made by cleaner

production containing hazardous waste were monitored. The testing within this research mainly involved monitoring changes in the properties of the grouts after the action of a chemically aggressive environment, with an emphasis on the study of characteristic parameters such as surface hardness, abrasion resistance and strength. These parameters simulated the usual synergistic effects of mechanical and chemical loads when using the system in real conditions. The testing was supplemented by the monitoring of the microstructure of the developed grouts, including after advanced chemical resistance testing (i.e. after simulation of a chemically aggressive environment in real conditions). The chemical resistance testing is significant for the prediction of the long-term durability of jointing grouts applied in sewers and industrial plants in which a strong chemically aggressive environment acts. It was found that the type of filler used in the form of a solidification product does not have a significant negative effect on the chemical resistance and glass transition temperature (T_g) of the resulting composite grout. Samples with incorporated FHW2 solidification products, on the other hand, achieved better physical–mechanical properties compared to reference grouts that are applied as a standard for grouting in chemically demanding environments. The grouts containing hazardous waste CBD have better properties due to the more suitable particle shape, dispersibility and anchorage in the epoxy matrix (stronger binder/filler contact zone) and the creation of a more compact structure, which results in lower diffusion of aggressive solutions into the internal structure. Newly developed jointing grouts made by cleaner production (utilisation of hazardous waste) have unique properties, display high chemical resistance, resist aggressive environments and can be used in a wide range of applications. It was proven that the new jointing grout ERG-D based on Novolac, epoxy resin containing phenol, shows the highest chemical resistance of all tested grouts, but in a humid environment without the need to dry the base. The results also support the use of jointing compound MRG-D, which is based on water compatible resins and shows a good degree of chemical resistance for the applications considered.

Acknowledgments

This research was supported by the project of Brno University of Technology, Faculty of Civil Engineering No. FAST-S-21-7228 “Analysis of the influence of the size and morphology of microfiller particles from primary and secondary raw materials on the resulting properties of composite materials” and by the project ADMATEC—Advanced Materials and Technologies, subproject of TN01000056 CAMEB— ‘Centre for Advanced Materials and Efficient Buildings’, grant number TN01000056/04.

References

[1] Z. Shi, S. Watanabe, K. Ogawa, H. Kubo, Domestic and global expansion of sewer reconstruction projects. In: Structural Resilience in Sewer Reconstruction (2018), pp. 421–464, https://doi.org/10.1016/B978-0-12-811552-7.00010-9.

[2] B. Simpson, N.A. Hoult, I.D. Moore, Rehabilitated reinforced concrete culvert performance under surface loading, Tunn. Undergr. Space Technol. 69 (2017), pp. 52–63, https://doi.org/10.1016/J.TUST.2017.06.007.

[3] N. Eliaz, E.Z. Ron, M. Gozin, S. Younger, D. Biran, N. Tal, Microbial degradation of epoxy, Materials 11 (11) (2018) 1–15. https://doi.org/10.3390/ma11112123.

[4] R. Drochytka, A. Jakubík, J. Hodul, T. Žlebek, Protection of the cast basalt sewers for enhancing resistance to biocorrosion, PROTECT 2019 Whistler, BC, Canada, September 16-17, 2019.

[5] X. Li, L. O'Moore, S. Wilkie, Y. Song, J. Wei, P.L. Bond, Z. Yuan, L. Hanzic, L., G. Jiang, Nitrite admixed concrete for wastewater structures: Mechanical properties, leaching behavior and biofilm development, Constr. Build. Mater. 233 (2020) 117341, https://doi.org/10.1016/j.conbuildmat.2019.117341.

[6] C. Yongsiri, J. Vollertsen, T. Hvitved-Jacobsen, Influence of Wastewater Constituents on Hydrogen Sulfide Emission in Sewer Networks. J. Environ. Eng. 131 (12) (2005), https://doi.org/10.1061/(ASCE)0733-9372(2005)131:12(1676).

[7] H. Bauer, M. Fuerhacker, F. Zibuschka, H. Schmid, H. Puxbaum, Bacteria and fungi in aerosols generated by two different types of wastewater treatment plants, Water Research 36 (16) (2002), pp. 3965–3970, https://doi.org/10.1016/S0043-1354(02)00121-5.

[8] M. Huang, Y. Li, G. Gu, Chemical composition of organic matters in domestic wastewater, Desalination 262 (1–3) (2010), pp. 36–42, https://doi.org/10.1016/j.desal.2010.05.037.

[9] M.G. Alexander, C. Fourie, Performance of sewer pipe concrete mixtures with portland and calcium aluminate cements subject to mineral and biogenic acid attack, Materials and Structures 44 (2011), pp. 313–330, https://doi.org/10.1617/s11527-010-9629-1.

[10] Z. Su, Z. Wang, D. Zhang, T. Wei, Study on rheological behavior and surface properties of epoxy resin chemical grouting material considering time variation, Materials 12 (20) (2019) 3277, doi:10.3390/ma12203277.

[11] Y. Bi, R. Li, S. Han, J. Pei, J. Zhang, Development and Performance Evaluation of Cold-Patching Materials Using Waterborne Epoxy-Emulsified Asphalt Mixtures, Materials 13 (5) (2020) 1224, doi:10.3390/ma13051224.

[12] H. Khoramishad, O. Alizadeh, Effects of silicon carbide nanoparticles and multiwalled carbon nanotubes on water uptake and resultant mechanical properties degradation of polymer nanocomposites immersed in hot water, Polym. Compos. 39 (2018), pp. E883–E890.

[13] X. Han, Y. Jin, W. Zhang, W. Hou, Y. Yu, Characterisation of moisture diffusion and strength degradation in an epoxy-based structural adhesive considering a postcuring process, J. Adhes. Sci. Technol. 32 (2018), pp. 1643–1657, https://doi.org/10.1080/01694243.2018.1436876.

[14] A. E. Sorokin, S.N. Bulychev, S.I. Gorbachev, Environmental impact of polymer composites, Russian Engineering Research 41 (2021), pp. 53-55, https://doi.org/10.3103/S1068798X21010214.

[15] X.N. Xia, X.L. Zeng, J. Liu, W.J. Xu, Preparation and characterization of epoxy/kaolinite nanocomposites, J. Appl. Polym. Sci. 118 (2010), pp. 2461–2466, https://doi.org/10.1002/app.32421.

[16] M. Oleksy, K. Szwarc-Rzepka, M. Heneczkowski, R. Oliwa, T. Jesionowski, Epoxy resin composite based on functional hybrid fillers, Materials 7 (8) (2014), pp. 6064–6091, https://doi.org/10.3390/ma7086064.

[17] Y. Rostamiyan, A.H. Mashhadzadeh, A. SalmanKhani, Optimization of mechanical properties of epoxy-based hybrid nanocomposite: Effect of using nano silica and high-impact polystyrene by mixture design approach, Mater. Des. 56 (2014), pp. 1068–1077, https://doi.org/10.1016/j.matdes.2013.11.060.

[18] M. Safiuddin, M.Z. Jumaat, M.A. Salam, M.S. Islam, R. Hashim, Utilization of solid wastes in construction materials, Int. J. Phys. Sci. 5 (13) (2010), pp. 1952–1963.

[19] B. Vacenovska, V. Cerny, R. Drochytka, B. Urbanek, E. Vodickova, J. Pavlikova, V. Valko, Verification of the possibility of solidification product made of neutralization sludge use in the building industry, Procedia Engineering 57 (2013), pp. 1192–1197, https://doi.org/10.1016/j.proeng.2013.04.150.

[20] T. Žlebek, J. Hodul, R. Drochytka, Polymer based grout with specially treated hazardous waste, IOP Conference Series: Materials Science and Engineering 549 (2019) 12030, https://doi:10.1088/1757-899X/549/1/012030.

[21] S. Zhao, B. Liu, Y. Ding, J. Zhang, Q. Wen, C. Ekberg, S. Zhang, Study on glass-ceramics made from MSWI fly ash, pickling sludge and waste glass by one-step process, J. Clean. Prod. 271 (2020) 122674. https://doi.org/10.1016/j.jclepro.2020.122674.

[22] A. Erdoğan, M.S. Gök, V. Koç, A. Günen, Friction and wear behavior of epoxy composite filled with industrial wastes, J. Clean. Prod. 237 (2019) 117588, https://doi.org/10.1016/j.jclepro.2019.07.063.

[23] H.M. Jafer, W. Atherton, M. Sadique, F. Ruddock, E. Loffill, Development of a new ternary blended cementitious binder produced from waste materials for use in soft soil stabilisation, J. Clean. Prod. 172 (2018), pp. 516–528, https://doi.org/10.1016/j.jclepro.2017.10.233.

[24] Y. Pan, J. Rossabi, C. Pan, X. Xie, Stabilization/solidification characteristics of organic clay contaminated by lead when using cement, J. Hazard Mater. 362 (2019), pp. 132–139, https://doi.org/10.1016/j.jhazmat.2018.09.010.

[25] B. Dohnálková, R. Drochytka, J. Hodul, New possibilities of neutralisation sludge solidification technology, J. Clean. Prod. 204 (2018), pp. 1097-1107, https://doi.org/10.1016/j.jclepro.2018.08.095.

[26] V. Massardier, P. Moszkowicz, M. Taha, Fly ash stabilization-solidification using polymer-concrete double mastrices, Eur. Polym. J. 33 (7) (1997), pp. 1081–1086, https://doi.org/10.1016/S0014-3057(96)80250-3.

[27] C. Vipulanandan, S. Krishnan, Solidification/Stabilization of phenolic waste with cementitious and polymeric materials, J. Hazard. Mater. 24 (2-3) (1990), pp. 123–136, https://doi.org/10.1016/0304-3894(90)87004-2.

[28] R.J.C. Carbas, E.A.S. Marques, L.F.M. Da Silva, A.M. Lopes, Effect of cure temperature on the glass transition temperature and mechanical properties of epoxy adhesives, The Journal of Adhesion 90 (2014), pp. 104-119, https:// 10.1080/00218464.2013.779559.

[29] S. Le Craz, R.A. Pethrick, Solvent effects on cure 1-benzyl alcohol on epoxy cure, Int. J. Polym. Mater. 60 (7) (2011), pp. 441-455.

[30] J. Ding, G. Sun, B. Liu, Synthesis of rubber vulcanization accelerator n-cyclohexyl-2-benzothiazolesulphenamide with crude 2-mercaptobenthiazole, Speciality Petrochem. 25 (2008), pp. 47-50

[31] J.L. Chen, F.C. Chang, Phase separation and melting behavior in poly(ε-caprolactone)-epoxy blends cured by 3,3'-dimethylmethylene-di(cyclohexylamine), J. Appl. Polym. Sci. 89 (2003), pp. 3107-3114, https://doi.org/10.1002/app.12499.

[32] J.M. Kenny, A. Apicella, L. Nicolais, A model for the thermal and chemorheological behavior of thermosets. I: Processing of epoxy-based composites, Polym. Eng. Sci. 1989 29 (1989), pp. 973-983.

[33] C. Lanzerstorfer, Residue from the chloride bypass de-dusting of cement kilns: Reduction of the chloride content by air classification for improved utilisation, Process Saf. Environ. Prot. 104 (A) (2016), pp. 444–450, https://doi.org/10.1016/j.psep.2016.06.010.

[34] J. Hodul, L. Mészárosová, T. Žlebek, R. Drochytka, Z. Dufek, Impact of Aggressive Media on the Properties of Polymeric Coatings with Solidification Products as Fillers, Coatings 9 (12) (2019) 793, https://doi.org/10.3390/coatings9120793.

[35] K. Shi-Cong, P. Chi-Sun, A novel polymer concrete made with recycled glass aggregates, fly ash and metakaolin, Constr. Build. Mater. 41 (2013), pp. 146-151, http://dx.doi.org/10.1016/j.conbuildmat.2012.11.083.

[36] K.T. Varughese, B.K. Chaturvedi, Fly ash as fine aggregate in polyester based polymer concrete. Cem. Concr. Compos. 18 (1996), pp. 105–108, https://doi.org/10.1016/0958-9465(95)00006-2.

[37] S. Sugiman, I.K.P. Putra, P.D. Setyawan, Effects of the media and ageing condition on the tensile properties and fracture toughness of epoxy resin, Polymer Degradation and Stability 134 (2016), pp. 311-321, https://doi.org/10.1016/j.polymdegradstab.2016.11.006.

[38] M. Vyšvařil, M. Rovnaníková, Sulfuric acid attack on various types of fine grained concrete, Adv. Mat. Res. 1100 (2015), pp. 101–105, https://doi.org/10.4028/www.scientific.net/AMR.1100.101.

[39] EN 13892-3:2014, Methods of test for screed materials - Part 3: Determination of wear resistance – Böhme, European Committeefor Standardization (CEN), Brussels, Belgium, 2014.

[40] EN 12808-3, Grouts for tiles. Determination of flexural and compressive strength, European Committee for Standardization (CEN), Brussels, Belgium, 2008.

[41] P. Kalenda, Chemical-resistance values of epoxy resins hardened with polyamines, Pigment & Resin Technology 30 (3) (2001), pp. 150–158, https://doi.org/10.1108/03699420110390797.

[42] A. Wegmann, Chemical resistance of waterborne epoxy/amine coatings, Prog. Org. Coat. 32 (1–4) (1997) 231–239, https://doi.org/10.1016/S0300-9440(97)00062-3.

[43] H.G. Cooke, A.R. Strohscher, W.F. McWhorter, Chemical resistance of epoxy resins, Industrial and Engineering Chemistry 56 (5) (1964), pp. 38–41, https://doi.org/10.1021/ie50653a005.

[44] M. Zhang, B. Sun, B. Gu, Accelerated thermal ageing of epoxy resin and 3-D carbon fiber/epoxy braided composites, Composites Part A : Applied Science and Manufacturing 85 (2016), pp. 163-171, https://doi.org/10.1016/j.compositesa.2016.03.028.

[45] G.L. de Oliveira, A.J.A. Gomez, M. Caire, M.A. Vaz, M.F. da Costa, Characterization of seawater and weather aged polyurethane elastomer for bend stiffeners, Polym. Test. 59 (2017), pp. 290–295, https://doi.org/10.1016/j.polymertesting.2017.02.012.

[46] M. Mozzami, M.R. Ayatollahi, A. Akhavan-Safar, L.F.M. da Silva, Experimental and numerical analysis of cyclic aging in an epoxy-based adhesive, Polymer Testing 91 (2020) 106789, https://doi.org/10.1016/j.polymertesting.2020.106789.

[47] J. Zhang, Y.C. Xu, P. Huang, Effect of cure cycle on curing process and hardness for epoxy resin, eXPRESS Polymer Letters 13 (9) (2009), pp. 534-541, https://doi.org/10.3144/expresspolymlett.2009.67.

[48] C.V. Srinvasa, K.N. Bharath, Impact and Hardness Properties of Areca Fiber-Epoxy Reinforced Composites, J. Mater. Environ. Sci. 2 (4) (2011), pp. 351-356.

[49] M. Lettieri, M. Frigione, Effects of humid environment on thermal and mechanical properties of a cold-curing structural epoxy adhesive, Constr. Build. Mater. 30 (2012), pp. 753-760, 10.1016/j.conbuildmat.2011.12.077.

[50] M.C.S. Ribeiro, C.M.L. Tavares, A.J.M. Ferreira, Chemical resistance of epoxy and polyester polymer concrete to acids and salts, Journal of polymer engineering 22 (1) (2002), pp. 27–44, https://doi.org/10.1515/POLYENG.2002.22.1.27.

[51] S. Mebarkia, C. Vipulanandan, Mechanical properties and water diffusion in polyester polymer concrete, J. Eng. Mech. 121 (12) (1995), pp. 1359–1365, https://doi.org/10.1061/(ASCE)0733-9399(1995)121:12(1359).

[52] J.M. Sousa, J.R. Correia, S. Cabral-Fonseca, Durability of an epoxy adhesive used in civil structural applications, Constr. Build. Mater. 161 (2018), pp. 618-633, https://doi.org/10.1016/j.conbuildmat.2017.11.168.

[53] M.Y. Fard, Nonlinear inelastic mechanical behaviour of epoxy resin polymeric materials, A dissertation presented in partial fulfilment of the requirements for the degree doctor of philosophy, Arizona state university, August 2011, p. 192.

[54] M. Mozzami, M.R. Ayatollahi, A. Akhavan-Safar, L.F.M. da Silva, Experimental and numerical analysis of cyclic aging in an epoxy-based adhesive, Polymer Testing 91 (2020) 106789, https://doi.org/10.1016/j.polymertesting.2020.106789.

[55] P. Nogueira, C. Ramírez, A. Torres, M.J. Abad, J. Cano, J. López, et al., Effect of water sorption on the structure and mechanical properties of an epoxy resin system, J. Appl. Polym. Sci. 80 (2001), pp. 71–80.

[56] A.J. Lesser, E. Crawford, The role of network architecture on the glass transition temperature of epoxy resin, Journal of Applied Polymer Science 66 (1997), pp. 387-395.

[57] G. Liang, A. Garg, K. Chandrashekhara, K., V. Flanigan, S. Kapila, Cure characterization of pultruded soy-based composites, J. Reinf. Plast. Compos. 24 (2005), pp. 1509-1520, https://doi.org/10.1177/0731684405050387.

[58] G. Liang, K. Chandrashekhara, Cure kinetics and rheology characterization of soy-based epoxy resin system, Journal of Applied Polymer Science 102 (4) (2006), pp. 3168-3180, https://doi.org/10.1002/app.24369.

[59] L. Li, M. Liu, S. Li, Morphology effect on water sorption in a thermoplastic modified epoxy system, Polymer 45 (2004), pp. 2837-2842, https://doi.org/10.1016/j.polymer.2004.02.002.

[60] L. Li, Y. Yu, Q. Wu, G. Zhan, S. Li, Effect of chemical structure on the water sorption of amine-cured epoxy resins, Corros. Sci. 51 (2009), pp. 3000-3006, https://doi.org/10.1016/j.corsci.2009.08.029.

[61] W.K. Loh, A.D. Crocombe, M.M.A. Wahab, I.A. Ashcroft, Modelling anomalous moisture uptake, swelling and thermal characteristics of a rubber toughened epoxy adhesive, Int. J. Adhes. Adhes. 25 (2005), pp. 1-12.